
AN INVESTIGATION OF ROBUSTNESS OF LLMs IN MATHEMATICAL REASONING: BENCHMARKING WITH MATHEMATICALLY-EQUIVALENT TRANSFORMATION OF ADVANCED MATHEMATICAL PROBLEMS

Yuren Hao

Department of Computer Science
University of Illinois Urbana-Champaign
Urbana, IL, USA
yurenh2@illinois.edu

Xiang Wan

Department of Data Science
Stanford University
Stanford, CA, USA
oscarwan@stanford.edu

ChengXiang Zhai

Department of Computer Science
University of Illinois Urbana-Champaign
Urbana, IL, USA
czhai@illinois.edu

ABSTRACT

In this paper, we introduce a systematic framework beyond conventional method to assess LLMs’ mathematical-reasoning robustness by stress-testing them on advanced math problems that are mathematically equivalent but with linguistic and parametric variation. These transformations allow us to measure the sensitivity of LLMs to non-mathematical perturbations, thereby enabling a more accurate evaluation of their mathematical reasoning capabilities. Using this new evaluation methodology, we created PutnamGAP, a new benchmark dataset with multiple mathematically-equivalent variations of competition-level math problems. With the new dataset, we evaluate multiple families of representative LLMs and examine their robustness. Across 18 commercial and open-source models we observe sharp performance degradation on the variants. OpenAI’s flagship reasoning model, O3, scores 51.5 % on the originals but drops by 4.7 percentage points on surface-renaming variants, and by 12.9 percentage points on parametric variants, while smaller models fare far worse. Overall, the results show that the proposed new evaluation methodology is effective for deepening our understanding of the robustness of LLMs and generating new insights for further improving their mathematical reasoning capabilities.

1 Introduction

Motivation. Modern AI systems are increasingly entrusted with tasks that hinge on robust reasoning rather than pattern matching. It is thus important to precisely measure an LLM’s reasoning capacity and its ability to generalize beyond memorized textual surface forms. Existing math-reasoning benchmarks, however, exhibit two critical weaknesses: (i) leakage-induced score inflation, since benchmark items rapidly seep into pre-training corpora, and (ii) limited robustness coverage, because today’s datasets are too small or lack controlled transformations that probe true generalization. Addressing these weaknesses is urgent if we aim to benchmark reasoning with the same rigor demanded in safety-critical domains such as healthcare or cybersecurity.

Benchmark inflation through training leakage. Recent studies show that public datasets, including GSM8K (Cobbe et al., 2021) and MATH (Hendrycks et al., 2021), have leaked into the web-scale corpora used to pre-train large language models (LLMs), artificially inflating test-time accuracy. A leaderboard score therefore no longer guarantees genuine reasoning ability; it may merely reflect memorization of benchmark items or their solutions. Simply releasing *yet another*

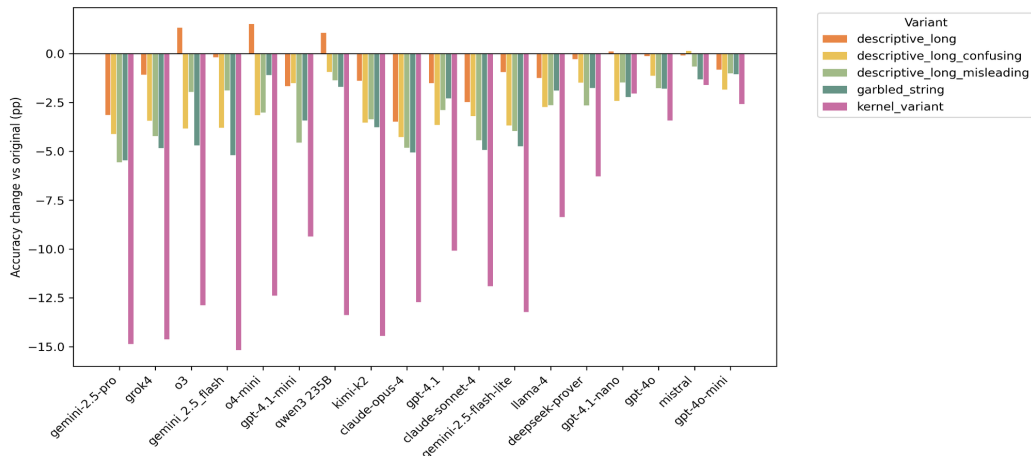


Figure 1: PutnamGAP variants performance relative to the original set

dataset postpones the problem: once its items enter future training corpora, scores climb without real progress. What is needed is a *systematic method* that (i) measures a model’s capacity to generalize beyond verbatim memory and (ii) can generate an unbounded supply of evaluation items, limiting future leakage.

Competition mathematics reveals the next robustness bottleneck. Large language models (LLMs) now surpass 90% accuracy on widely-used benchmarks such as GSM8K and MATH, prompting claims of “near-human” numerical reasoning yet still falter on Olympiad-style or Putnam-level problems that intertwine multiple domains. Existing Putnam-derived datasets are too small to expose this gap: PUTNAM-AXIOM (236 originals + 52 variations) (Huang et al., 2025), and PUTNAMBENCH (640 formalized theorems) (Tsoukalas et al., 2024) remain in the hundreds, and none delivers systematic generalization and perturbations. These facts expose Weakness (i) insufficient scale and Weakness (ii) lack of controlled, systematic transformations in existing evaluations.

Generalization-and-Perturbation (GAP), a novel evaluation strategy. We address both leakage and robustness with a new idea: *stress-test the model on mathematically equivalent versions of the same problem*. For a problem x with solution set $S(x)$ and an LLM f , robustness is the expected accuracy when x is transformed by a family \mathcal{T} of equivalence-preserving operators. We partition \mathcal{T} into $\mathcal{T}_{\text{surf}}$ (surface renames that alter symbol salience) and $\mathcal{T}_{\text{para}}$ (kernel rewrites that preserve the same proof steps while changing the scenario and parameters). This **GAP** framework (i) creates an *infinite* stream of *unseen* test items, mitigating future contamination, and (ii) quantifies how far a model can generalize beyond memorized surface forms. It offers a new general diagnostic evaluation methodology for analyzing and quantifying the robustness of an LLM’s mathematical reasoning capacity.

PutnamGAP: instantiating GAP on 85 years of problems. We instantiate GAP on every William Lowell Putnam Competition problem from 1938–2024 (**1,051** originals) and expand each item into five variants—four surface renames and one kernel rewrite—obtaining **6,306** stress-test questions. A two-stage QA pass—15 rounds of o3 self-review plus a 10% spot-check found no substantive errors.

Headline results. Across 18 models, as shown figure 4, all of them suffer from both simple renaming and step-based rewrites. OpenAI’s o3 scores 51.5% on original statements but loses **4.7 pp (9.12%)** under surface renames and **12.9 pp (25.22%)** under parametric rewrites. These drops confirm that high leaderboard scores can collapse when cosmetic or structural perturbations are applied—precisely the effect that data leakage masks.

Contributions. (1) We propose *GAP*, a novel general framework for measuring robustness via mathematically equivalent transformations that overcomes two common deficiencies of the current evaluation methods (i.e., data leakage and lack of robustness measures). (2) We release *PutnamGAP*, the first 6k-scale competition benchmark that systematically disentangles surface-level and structural

generalization while limiting future leakage. (3) We provide the first comprehensive robustness baseline across seventeen LLMs, plus an open-source evaluation stack.

2 The Generalization-and-Perturbation (GAP) Framework

2.1 Evaluation Model

We start from a curated set of N canonical items $\mathcal{P} = \{(x_i, y_i, \pi_i)\}_{i=1}^N$, where x_i is a problem statement, y_i is its reference answer(s), and π_i an unreleased expert solution path used internally for safe variant generation. **Model interface.** A language model f_θ receives a prompt x and returns $\hat{y} = f_\theta(x)$, which an automatic checker maps to a binary label $z = \text{grade}(\hat{y}, y) \in \{0, 1\}$.

Variant families. For every x_i we later apply *two* disjoint transformation super-families (defined in the next section but *left unchanged here*): $\mathcal{T}_i^{\text{surf}}$ (K_{surf} surface variants), $\mathcal{T}_i^{\text{para}}$ (K_{para} parametric variants). Each surface transformation τ returns a new statement $x_i^{(\tau)} = \tau(x_i)$ that preserves semantic correctness of y_i . For parametric variations, y_i is transformed as well to match $\tau(x_i)$.

Evaluation matrix. The Cartesian product $\mathcal{D} = \{(i, \tau) \mid i \leq N, \tau \in \mathcal{T}_i^{\text{surf}} \cup \mathcal{T}_i^{\text{para}} \cup \{\text{id}\}\}$ contains $N \times (K + 1)$ aligned items (original + K variants per source, $K = K_{\text{surf}} + K_{\text{para}}$). Running f_θ on every pair populates a binary matrix $\mathbf{Z} \in \{0, 1\}^{N \times (K+1)}$. From the first column we extract the *easy* vector $\mathbf{e}(\theta) \in \{0, 1\}^N$, while the remaining columns feed family-specific aggregates: $\mathbf{h}^{\text{surf}}(\theta) = \text{maj}(\mathbf{Z}_{[:, \text{surf}]})$, $\mathbf{h}^{\text{para}}(\theta) = \mathbf{Z}_{[:, \text{para}]}$. The set of surface variants can be changed based on specific tasks.

Robustness Metric. Let $e, h \in \{0, 1\}^N$ denote per-item correctness on the *easy* (original) and *hard* (variant) sets. With Jeffreys smoothing

$$p_e = \frac{\sum_j e_j + \frac{1}{2}}{N + 1}, \quad p_h = \frac{\sum_j h_j + \frac{1}{2}}{N + 1}, \quad \sigma = \sqrt{\frac{1}{2}(p_e(1 - p_e) + p_h(1 - p_h))}.$$

Define the SD-normalized drop $d_j = (e_j - h_j)/\sigma$ and its soft-saturated version $\hat{d}_j = \frac{1}{k} \log(1 + e^{kd_j})$ with $k \approx 0.5$. Let $\tilde{d} = \text{median}\{d_j \mid d_j > 0\}$ (with fallback $\tilde{d} := \max(\varepsilon, \text{median}\{|d_j|)\}$, $\varepsilon = 0.1$ when no positive drop exists) and set $\beta = \ln 2/\tilde{d}$. Our *penalty* robustness is

$$\hat{R}(e, h) = \frac{1}{N} \sum_{j=1}^N \exp(-\beta \hat{d}_j) \in (0, 1].$$

Thus $\hat{R} = 1$ indicates invariance; a “typical” loss ($\hat{d}_j \approx \tilde{d}$) halves the per-item factor, while improvements ($d_j < 0$) are clamped to zero penalty (no reward). We report $R_{\text{surf}} = \hat{R}(e, h_{\text{surf}})$, $R_{\text{para}} = \hat{R}(e, h_{\text{para}})$, and $R_{\text{global}} = \sqrt{R_{\text{surf}} R_{\text{para}}}$. **Full derivation, statistical justification, and design discussion are in Appendix B.**

2.2 Transformation Families

The proposed general robustness measures can work for any variations. As a first step in exploring this new evaluation methodology, we propose and study *five* aligned variants—four *surface renamings* that perturb only symbol names, and one *core-step* instance that perturbs numeric slots while preserving the reasoning chain. This section details the synthesis pipelines. Detailed descriptions can also be found in Appendix A.

2.2.1 Surface renaming variant family

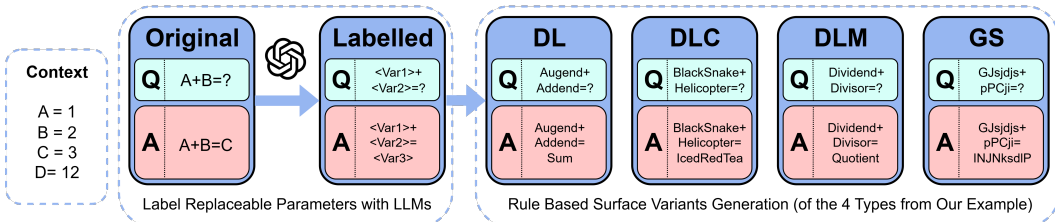


Figure 2: Surface renaming variant family pipeline

We want to know whether a model recognizes an argument *because it has truly abstracted the pattern* or merely because it memorizes suggestive identifier strings. Therefore we systematically replace each token tagged `var` or `param`; all constants of category `sci_const` remain untouched.

Automated pipeline.

- 1. Proposal.** A single call to O3 receives the token role (“free variable” or “fixed parameter”) and the surrounding textual context, and returns a candidate replacement.
- 2. Collision check.** A deterministic post-validator rejects names colliding with any pre-existing identifier in the problem.
- 3. Family tagging.** The string is labelled as belonging to one of four families described below.

We use four types of surface variants: `Descriptive_Long` (DL), with a single descriptive phrase; `Descriptive_Long_Confusing` (DLC), with 2–5 random unrelated nouns; `Descriptive_Long_Misleading` (DLM), with a mathematically suggestive but misleading term; `Garbled_String` (GS), with a 4–16-character hash, as shown in figure 2 where ‘Q’ stands for the problem question and ‘A’ stands for the official solution.

Each source item thus yields 4 surface variants; accuracy deltas per family appear in Section Results & Analysis.

2.2.2 Parametric variant family

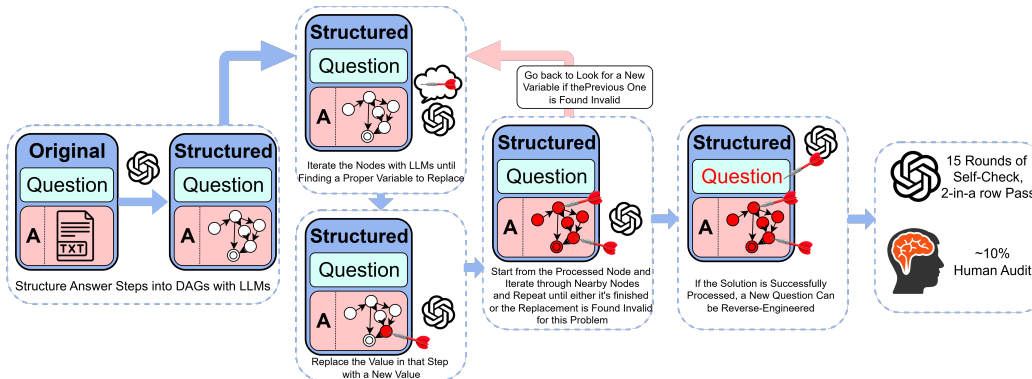


Figure 3: Parametric variant family pipeline

Symbol renaming probes only the lexical axis. To probe *structural transfer*, we resample numerical constants yet force the solution to reuse the original high-level moves. In this work, we call it `Kernel_Variant` (KV). We convert each item into semantically-equivalent variants through a four-stage pipeline: (1) **slot discovery**; (2) **template back-synthesis**; (3) **question reverse-engineering**; and (4) **dual-verifier screening** (two-in-a-row rule). The pipeline generates a bounded number of validated variants for each problem within a few hours on commodity hardware using the OpenAI o3 API. See Appendix A for empirical bounds and details of our implementation.

2.3 Implementation Overview

Code release. To facilitate double-blind reviewing we publish *only* the subset of data (100 randomly chosen examples). An automated evaluator, `putnam-cli.py`, receives the names of target solver model and grader model and variant type to test. Supported back-ends are (i) any HuggingFace-compatible checkpoint via `transformers`, (ii) a local `vllm` server, or (iii) API clients including OpenAI, Gemini, Anthropic and OpenRouter. Full data and generation scripts will be released post-decision.

Surface generation. Renaming variants are produced on a CPU-only node by streaming O3 API calls. A five-stage *exponential-back-off* retry (max 5 attempts, doubling timeout each time) masks transient API latency. Processing all 1 051 items in parallel takes ~15 min wall-clock.

Core-step generation. Kernel variant synthesis is more expensive because of multi-turn chain-of-thought reasoning: end-to-end runtime is ≤ 3 h for the full corpus on a single 8-core CPU, dominated by the 15-iteration repair-and-verify loop.

3 PutnamGAP Dataset

3.1 Data Sources, Extraction & Annotation

Our benchmark comprises all **Putnam Problems 1938–2024** ($N = 1\,051$ items after deduplication). See Appendix E for source details.

Original scans are processed via a 3-stage OCR routine: (i) Manual segmentation for every question-answer pair. (ii) *MathPix* for formula-aware PDF-to-LaTeX conversion followed by (iii) custom post-filters that merge multi-line expressions and fix 4.2 % residual symbol errors. Each item is manually spot-checked (≤ 2 min per problem) to ensure semantic fidelity before variant generation. **Complete corpus list, OCR accuracy study, and cleaning scripts appear in Appendix E.**

3.2 Dataset Statistics

Overall scale and balance. The benchmark comprises **1,051** original Putnam problems from 1938–2024 and five mathematically equivalent transformations, yielding **6,306** items. Part distribution is balanced (**527 A** vs. **524 B**), and the canonical identifier $\langle year, part\{A, B\}, index \rangle$ provides a difficulty proxy. Using indices 1–2 as *Easy*, 3–4 as *Medium*, and 5–6 as *Hard*, the corpus contains 32.3 % Easy, 32.3 % Medium, 32.2 % Hard, plus a 3.0 % extra-hard tail (indices 7–8).

Topic coverage and Quality Control Automatic tags in `_meta.tag` indicate broad mathematical coverage—Algebra (641), Analysis (521), Number Theory (392), Combinatorics (286), and Geometry (239). 803 of the questions are proofs, and 248 of them are calculations. At the same time, every item has undergone single-pass manual validation.

4 Experimental Setup

The constructed PutnamGAP dataset enables, for the first time, a robust analysis of an LLM’s reasoning capacity. In this section, we describe how we set up the experiments to evaluate the robustness of 18 representative models.

4.1 Model Pool & Prompting

We evaluated 18 models (see 1 or Appendix A for a complete list). All models are queried under a unified **zero-shot template**. A system instruction designates the model as “*an expert mathematician*” and asks it to *show all work*, while the user message embeds the problem. See Appendix G for our full prompt. We fix `temperature=0`, `top_p=1`, and `max_tokens=32000` or maximum token amount available in case some models have `max_tokens` maximum smaller than 32000. for every run except OpenAI O-series which require `temperature=1`. Solutions are then re-submitted to a second template that grades the answer: a STRICT PROOF RUBRIC for proof items and a LENIENT NUMERIC RUBRIC for calculation items. Both grader prompts require structured JSON output containing a binary `grade` field plus detailed feedback. Complete prompt code is available in Appendix G

4.2 Scoring & Auto-Grader

We partition tasks into *computation* and *proof* categories and evaluate them with distinct graders.

Computation Each candidate answer is normalized (whitespace, units, LaTeX macros) and passed to two scoring paths: (i) a strict string match against the reference solution; (ii) a *latent* grader—an LLM prompted to return ‘‘CORRECT’’ or ‘‘INCORRECT’’ given the reference answer and a rubric that disallows partial credit. We adopt path (ii) to mitigate formatting artifacts; if the two paths disagree we mark the item for manual audit ($\approx 1\%$ of cases).

Proof We provide the grader with an aligned, step-by-step reference proof and ask it to assign a binary `grade` plus a natural-language justification. Any skipped logical step or missing citation triggers a fail. A random 10 % sample is double-checked by independent volunteers; grader precision/recall is $>97\%$.

Table 1: Model Accuracy Rates across Categories (Percent Scale)

| Model | DL (Δ) | DLC(Δ) | DLM (Δ) | GS (Δ) | Kernel Variant (Δ) |
|-----------------------|-----------------|-----------------|------------------|-----------------|-----------------------------|
| claude-opus-4 | 23.0** (-3.5) | 22.2*** (-4.3) | 21.7*** (-4.8) | 21.4*** (-5.1) | 13.8*** (-12.7) |
| claude-sonnet-4 | 20.6** (-2.5) | 19.8*** (-3.2) | 18.6*** (-4.4) | 18.1*** (-4.9) | 11.1*** (-11.9) |
| deepseek-prover | 15.2 (-0.3) | 14.0 (-1.5) | 12.8** (-2.7) | 13.7* (-1.8) | 9.2 *** (-6.3) |
| gemini-2.5-flash-lite | 18.8 (-0.9) | 16.1*** (-3.7) | 15.8*** (-4.0) | 15.1*** (-4.7) | 6.6 *** (-13.2) |
| gemini-2.5-pro | 75.2** (-3.1) | 74.3*** (-4.1) | 72.8*** (-5.6) | 72.9*** (-5.4) | 63.5*** (-14.9) |
| gemini-2.5-flash | 42.6 (-0.2) | 39.0*** (-3.8) | 40.9 (-1.9) | 37.6*** (-5.2) | 27.6*** (-15.2) |
| gpt-4.1 | 23.4 (-1.5) | 21.2** (-3.7) | 22.0* (-2.9) | 22.6 (-2.3) | 14.8*** (-10.1) |
| gpt-4.1-mini | 26.9* (-1.7) | 27.1 (-1.5) | 24.0*** (-4.6) | 25.1** (-3.4) | 19.2*** (-9.4) |
| gpt-4.1-nano | 8.9 (+0.1) | 6.4 ** (-2.4) | 7.3 * (-1.5) | 6.6 ** (-2.2) | 6.8 (-2.0) |
| gpt-4o | 6.3 (-0.1) | 5.3 ** (-1.1) | 4.7 ** (-1.8) | 4.7 *** (-1.8) | 3.0 *** (-3.4) |
| gpt-4o-mini | 3.5 (-0.8) | 2.5 *** (-1.8) | 3.3 (-1.0) | 3.2 (-1.1) | 1.7 *** (-2.6) |
| grok4 | 59.0 (-1.1) | 56.6 (-3.4) | 55.9*** (-4.2) | 55.2*** (-4.8) | 45.5*** (-14.6) |
| kimi-k2 | 25.8 (-1.4) | 23.7** (-3.5) | 23.8** (-3.4) | 23.4*** (-3.8) | 12.8*** (-14.4) |
| llama-4 | 14.5 (-1.2) | 13.0** (-2.7) | 13.1** (-2.6) | 13.8* (-1.9) | 7.3 *** (-8.4) |
| mistral | 5.5 (-0.1) | 5.7 (+0.1) | 4.9 (-0.7) | 4.2 * (-1.3) | 3.9 * (-1.6) |
| o3 | 52.8 (+1.3) | 47.6** (-3.8) | 49.5 (-2.0) | 46.8*** (-4.7) | 38.6*** (-12.9) |
| o4-mini | 43.0 (+1.5) | 38.3** (-3.2) | 38.5 (-3.0) | 40.4 (-1.1) | 29.1*** (-12.4) |
| qwen3 | 29.3 (+1.1) | 27.3 (-0.9) | 26.9 (-1.4) | 26.5 (-1.7) | 14.9*** (-13.4) |

Note: *** $p < 0.01$, ** $p < 0.05$, * $p < 0.1$

5 Results & Analysis

5.1 Robustness

We evaluated 18 different LLMs on this benchmark, and results are summarized in Table 1. For each variation of the model, we used a paired design (McNemar’s exact test) on matched problem pairs to test whether the accuracy rate decreases significantly compared to the original. Statistically significant differences are indicated using standard notation ($p < 0.1$, $p < 0.05$, $p < 0.01$). We also computed 95 % CI (See Appendix D Figure 4) and robustness metrics R (See Appendix D Figure 9), and all models, especially those performed well on the original set, got a low robustness score.

We observe that almost all variants lead to a decrease in model accuracy, even when the transformation is merely changing the names of the variables. This indicates a notable lack of robustness: models often lack the capability to preserve their accuracy under mathematically identical but surface-modified representations. Particularly, transformations that rely on variable-name reasoning (such as Misleading or Garbled String) tend to disturb the model’s math accuracy most severely.

Table 2: Robustness metrics R_{surf} , R_{para} , R_{global} (rounded to three decimals).

| Model | R_{surf} | R_{para} | R_{global} | Model | R_{surf} | R_{para} | R_{global} |
|-----------------------|-------------------|-------------------|---------------------|-------------|-------------------|-------------------|---------------------|
| claude-opus-4 | 0.958 | 0.949 | 0.954 | gpt-4o | 0.986 | 0.980 | 0.983 |
| claude-sonnet-4 | 0.961 | 0.942 | 0.951 | gpt-4o-mini | 0.990 | 0.986 | 0.988 |
| deepseek-prover | 0.972 | 0.960 | 0.966 | grok4 | 0.937 | 0.916 | 0.927 |
| gemini-2.5-flash-lite | 0.961 | 0.942 | 0.952 | kimi-k2 | 0.955 | 0.930 | 0.942 |
| gemini-2.5-pro | 0.949 | 0.915 | 0.932 | llama-4 | 0.972 | 0.955 | 0.963 |
| gemini_2.5_flash | 0.952 | 0.918 | 0.934 | mistral | 0.984 | 0.982 | 0.983 |
| gpt-4.1 | 0.963 | 0.944 | 0.954 | o3 | 0.940 | 0.921 | 0.930 |
| gpt-4.1-mini | 0.953 | 0.939 | 0.946 | o4-mini | 0.946 | 0.929 | 0.937 |
| gpt-4.1-nano | 0.980 | 0.982 | 0.981 | qwen3 | 0.941 | 0.928 | 0.934 |

Because the surface score aggregates four renaming variants by per-item majority, the flip probability from original to the aggregated surface set is suppressed; accordingly $R \approx 1$ is expected and should be read as an **upper-boundish** surface invariance (see 2). The user may implement any mapping functions based on their model performance while retain this core section. Across capable models we consistently observe $R_{\text{para}} < R_{\text{surf}}$, and we summarize stress-type invariance via $R_{\text{global}} = \sqrt{R_{\text{surf}}R_{\text{para}}}$. Interpreting $1 - R$ as a penalty mass highlights nontrivial fragility even when raw accuracy is high. Conversely, for weak models a high R is not evidence of robustness: when base accuracy p_e is small, the pooled SD $\sigma = \sqrt{\frac{1}{2}(p_e(1 - p_e) + p_h(1 - p_h))}$ and the bound

$1 - R \leq \min\{p_e, 1 - p_h\} (1 - q)$ with $q = \exp(-\beta d_{b+})$ limit the observable penalty, so $R \rightarrow 1$ reflects low headroom rather than invariance. Reporting both accuracy and $\{R_{\text{surf}}, R_{\text{para}}, R_{\text{global}}\}$ therefore stabilizes cross-model comparison under mathematically equivalent stress and shows that robustness remains limited despite strong performance on canonical phrasing. When base accuracy p_e is small, the pooled SD σ caps the observable penalty and the bound $1 - R \leq \min\{p_e, 1 - p_h\} (1 - q)$ with $q = \exp(-\beta d_b^+)$ (where d_b^+ denotes the positive part of the soft-saturated drop) implies that $R \rightarrow 1$ can reflect *low headroom* rather than invariance; we therefore report both accuracy and $\{R_{\text{surf}}, R_{\text{para}}, R_{\text{global}}\}$ for stable cross-model comparison.

Another observation is if a model is not robust on one variant, it tends to be not robust on other variants. Notable examples would be kimi-k2, cluase-opus-4 and gemini-2.5-pro.

5.2 Transformation-wise Breakdown

Descriptive Long (DL) The impact of this transformation is smallest overall: drops are marginal and mostly not significant. Some models such as o3 (+1.3), o4-mini(+1.5), and Qwen3-235B (+1.1) even improved slightly. This indicates that descriptive renaming preserving accuracy.

Confusing (DLC) Long, semantically meaningless variable names moderately reduce accuracy. Models like Claude-opus-4 (-4.3***) and GPT-4o-mini (-1.8***) showed significant drops.

Misleading (DLM) Replacing variables with misleading strings strongly hurts math accuracy. Nearly all models experienced a significant drop. Notably, Claude-Opus-4 (-4.8***), Gemini-2.5-pro (-5.6***), and Claude-Sonnet-4 (-4.4***) were among the most heavily affected.

Garbled String (GS) Random character strings consistently degrade performance: every model loses accuracy, over half significantly. Models such as Gemini-2.5-pro (-5.4***), Claude-Sonnet-4 (-4.9***), and Gemini-2.5-flash-lite (-4.7***) suffered the largest declines.

Kernel Variant (KV) Kernel variants—which keep each question’s mathematical structure but replace constants and expressions with different values—led to the sharpest decline overall. All models experienced large drops, often in the range of -5 to -15 points, with Grok4 (-14.6***), Gemini-2.5-flash (-15.2***), and Gemini-2.5-pro (-14.9***) showing the steepest declines.

Overall, state-of-the-art LLMs show inconsistent performance under semantics-preserving transformations and appear sensitive to superficial cues. This is consistent with the possibility that part of their gains reflects data-leakage-related memorization rather than stable mathematical reasoning. The pattern persists across topics and problem classes: bar plots with 95% CIs (Appendix D, fig. 4) and per-topic/per-class breakdowns (Appendix D, figs. 7-8) show similar robustness gaps across Algebra/Analysis/NT/Combinatorics/Geometry and for both proof and calculation items.

5.3 Error Taxonomy

Our grading script returns a brief comment for every incorrect answer. Using these comments, we grouped errors into four categories: *Symbol Confusion*, *Step Omission*, *Arithmetic*, and *Logic Hallucination*. Figure 5 in Appendix D shows that the relative frequency of these error types is nearly identical across variants; logic hallucinations dominate, accounting for roughly three-fifths of all wrong answers regardless of prompt wording. Thus, the accuracy drop is distributed across all categories rather than driven by a single one, confirming that mathematically equivalent perturbation consistently degrades LLM performance.

5.4 External Validation

We applied our surface-renaming protocols—**DLC** and **GS**—to ALG514 (kus, 2014). Accuracy decreased from Base 93.6% to DLC 90.9% ($\Delta = -2.7$ pp) and GS 89.3% ($\Delta = -4.3$ pp); McNemar tests (Base vs DLC: $b=24, c=10, p=0.024$; Base vs GS: $b=35, c=13, p=0.002$). These statistically significant drops indicate that GAP’s surface-renaming stress tests generalize to other math datasets and reveal nontrivial sensitivity to variable renaming.

6 Discussion

6.1 Key Findings

The proposed GAP framework allowed us to make the following new findings about the behavior of LLMs in performing mathematical reasoning:

Symbol-level perturbations cause substantial drops. Across the four *surface* variants—DL, DLC, DLM, and GS—merely renaming variables lowers accuracy by 3–5 pp on average; for example, GEMINI-2.5-PRO falls from 78.3% to 72.9% (−5.4 pp; see Table 1). This indicates that today’s SOTA models still rely on lexical “semantic anchors” rather than fully abstract proof structures.

Maintaining structure but resampling parameters is even harsher. The KERNEL VARIANT (KV) simultaneously resamples all mutable constants while preserving the original reasoning skeleton. Accuracy losses reach ≈ 10 pp; OPENAI O3 declines from 48.8% to 38.5% (−10.3 pp), showing that grasping a solution pattern does not automatically translate to parameter-invariant reasoning ability.

R_{global} reveals fine-grained brittleness. We compute $R_{\text{surf}}, R_{\text{para}}, R_{\text{global}}$ where $R(\cdot, \cdot)$ is the SD-normalized robustness metric. Because it exponentially penalizes rare but catastrophic flips, R_{global} tracks *effective* robustness more faithfully than a plain hard/easy accuracy ratio.

Takeaway. Across capable models we consistently observe $R_{\text{para}} < R_{\text{surf}}$, and we summarize stress-type invariance via $R_{\text{global}} = \sqrt{R_{\text{surf}}R_{\text{para}}}$; interpreting $1 - R$ as penalty mass highlights non-trivial fragility even when raw accuracy is high.

6.2 Implications

A novel evaluation methodology: The GAP framework provides a novel methodology for analyzing and evaluating the robustness of LLMs’ reasoning capacity by generating an (in principle) unbounded supply of semantically equivalent test items, which can limit future benchmark leakage and mitigate leaderboard inflation.

Improving robustness via curriculum fine-tuning: Our results suggest curriculum fine-tuning that explicitly randomizes (i) symbol identities and (ii) numeric parameters, instead of simply enlarging pre-training corpora. That is, we can leverage the GAP framework to augment data for fine-tuning a model to improve robustness.

Detecting potential security concerns: Surface-level fragility implies that production systems can be *prompt-injected* with mathematically innocuous renamings—highlighting the need to integrate robustness checks into red-team pipelines. Our evaluation framework enables such risk analysis before deploying any production system.

Reporting. We recommend reporting bootstrap CIs for R_b together with per-item histograms of SD-normalized drops $d_j = (e_j - h_j)/\sigma$; these visualize tail-risk (rare catastrophic flips) that raw accuracy masks and make robustness audits reproducible.

7 Related Work

There have been multiple benchmarks for evaluating the mathematical-reasoning capabilities of large language models (LLMs). Early math-reasoning benchmarks such as MATH(1.25 k problems) (Hendrycks et al., 2021), and GSM8K(8.5 k problems) (Cobbe et al., 2021), revealed basic arithmetic/algebra skills. But their difficulty is now saturated as LLMs scale. For instance, with prompting strategies such as DUP, GPT-4 attains 97.1% accuracy on GSM8K (Zhong et al., 2025). This ceiling at the high-school-competition level motivated the creation of a new generation of harder benchmarks.

Subsequent benchmarks target harder problems. OMNI-MATH contributes 4 428 rigorously annotated Olympiad-level problems (Gao et al., 2024). Likewise, OLYMPIADBENCH provides a bilingual, multimodal benchmark of 8 476 Olympiad-level math and physics problems with expert step-by-step solutions (He et al., 2024). The cross-disciplinary benchmark ARB consist questions in mathematics, physics, biology, chemistry, and law, with a rubric-based self-grading protocol (Sawada et al., 2023). Some other benchmarks focuses specifically on formal proof. MINIF2F

supplies 488 Olympiad-level problems formalized in multiple proof assistants (Zheng et al., 2022). PUTNAMBENCH, offers 1 692 rigorously hand-crafted formalizations of Putnam Competition problems (Tsoukalas et al., 2024).

Nevertheless, recent studies warn that scores on many NLP benchmarks may be artificially inflated by data contamination, when LLMs are trained on the benchmark questions. Sainz et al. (2023) point out that many benchmarks may be inflated because large language models often memorize test data seen during pre-training. Balloccu et al. (2024) conduct a systematic audit of data leakage for closed-source LLMs and estimate that roughly 4.7 million test examples from 263 datasets were likely exposed to the models.

In order to obtain a more robust evaluation of LLMs’ reasoning capabilities, it is important to prevent data leakage. One approach is to create original questions. FRONTIERMATH, for example, addresses this with a rigorously curated benchmark of hundreds of original, expert-level mathematics problems spanning fields from number theory to algebraic geometry (Glazer et al., 2024). PUTNAM-AXIOM takes this approach and comprises 522 challenging problems from the William Lowell Putnam Competition plus 100 programmatically generated functional variations, furnishing a contamination-resilient benchmark (Gulati et al., 2025).

Another method to deal with data leakage is introducing contrast sets—small, label-changing perturbations of existing test instances—to probe a model’s local decision boundary (Gardner et al., 2020). Huang et al. (2025) construct MATH-PERTURB that applies simple and hard perturbations to 279 level-5 MATH problems and discover that models suffer 12–16 percentage-point drops on the hard variant. Shalyt et al. (2025) complement this line of work with ASYMOB, a 17k-problem benchmark whose algebra-focused numerical and symbolic perturbations reveal performance drops of up to 70 percentage points, highlighting models’ fragility under such stress tests. Similarly, Yu et al. (2025) propose MATH-ROB, a synthetic benchmark that enables robustness evaluation against the data contamination through an instruction-based approach. These efforts either focus on specific aspects that limit generalizability, are based on benchmarks that are too easy for current models, or introduce transformations that are not mathematically equivalent, thus confounding true robustness evaluation.

Building on these prior efforts, our work introduces GENERALIZATION-AND-PERTURBATION (GAP), a unified framework that addresses both data leakage and robustness by generating mathematically equivalent variants of complex problems, significantly expanding the evaluation depth of existing benchmarks. The framework can be applied to existing and future benchmarks, and all types of questions to strengthen their reliability. To address the saturation of accuracy scores, we apply our framework to challenging, college-level competition mathematics problems. We instantiate GAP on every William Lowell Putnam Competition problem from 1938–2024 (1 051 originals), expanding each item into five mathematically equivalent variants and thereby producing PUTNAM-GAP, a corpus of 6,306 stress-test questions. Finally, we release an open-source evaluation stack that rigorously grades solutions step by step, making assessment fully automated, transparent, and reproducible.

8 Conclusion & Future Work

Robust reasoning is required in many applications of LLMs. In this paper, we proposed a novel **Generalization-and-Perturbation (GAP)** framework for analyzing and evaluating robustness of LLMs’ reasoning capacity. By instantiating GAP on *all* 1,051 Putnam Competition questions we produced the 6,306-question PUTNAMGAP benchmark. A zero-shot evaluation of 18 commercial and open-source LLMs revealed sharp and consistent accuracy drops. These results expose a clear robustness gap that leaderboard scores on unperturbed datasets have so far not shown.

Our findings highlight three actionable directions.

- *Benchmarking*: GAP offers an open-ended supply of contamination-resistant test items, limiting future data leakage and score inflation.
- *Training*: curricula that randomize both symbol identities and numeric parameters during fine-tuning should become standard practice for models targeting formal reasoning domains.
- *Security*: the same surface-level fragility that hurts accuracy can be weaponized for prompt-injection attacks, so GAP-style mutation should be built into red-teaming pipelines.

There are multiple interesting future research directions based on our work: (i) diversify the verifier ensemble with symbolic provers and heterogeneous LLMs to rule out collusive blind spots, (ii) port GAP to applied mathematics, physics and multi-modal STEM corpora, and (iii) integrate on-the-fly GAP transformations into training so that invariance to symbol and parameter changes is learned rather than merely tested.

PUTNAMGAP makes one lesson unmistakable: genuine progress in mathematical AI will be measured not by ever-higher raw scores, but by a model's ability to stride across the hidden gulf between *symbols* and *substance*. The next generation of top-tier systems will earn their place only by refusing to be left behind on GAPs.

References

- Learning to automatically solve algebra word problems”, author = ”kushman, nate and artzi, yoav and zettlemoyer, luke and barzilay, regina. In Kristina Toutanova and Hua Wu (eds.), *Proceedings of the 52nd Annual Meeting of the Association for Computational Linguistics (Volume 1: Long Papers)*, Baltimore, Maryland, June 2014. Association for Computational Linguistics. doi: 10.3115/v1/P14-1026. URL <https://aclanthology.org/P14-1026/>.
- Gerald L. Alexanderson, Leonard F. Klosinski, and Loren C. Larson. *The William Lowell Putnam Mathematical Competition: Problems and Solutions 1965–1984*, volume 30 of *MAA Problem Books*. Mathematical Association of America, Washington, DC, 1985. Reprinted by AMS/MAA Press.
- Simone Balloccu, Patrícia Schmidtová, Mateusz Lango, and Ondřej Dušek. Leak, cheat, repeat: Data contamination and evaluation malpractices in closed-source LLMs. In *Proceedings of the 18th Conference of the European Chapter of the Association for Computational Linguistics (Volume 1: Long Papers)*, pp. 67–93, St. Julian’s, Malta, 2024. Association for Computational Linguistics. doi: 10.18653/v1/2024.eacl-long.5. URL <https://aclanthology.org/2024.eacl-long.5/>.
- Karl Cobbe, Vineet Kosaraju, Mohammad Bavarian, Mark Chen, Heewoo Jun, Lukasz Kaiser, Matthias Plappert, Jerry Tworek, Jacob Hilton, Reiichiro Nakano, Christopher Hesse, and John Schulman. Training verifiers to solve math word problems. arXiv:2110.14168, 2021. URL <https://arxiv.org/abs/2110.14168>.
- Bofei Gao, Feifan Song, Zhe Yang, Zefan Cai, Yibo Miao, Qingxiu Dong, Lei Li, Chenghao Ma, Liang Chen, Runxin Xu, Zhengyang Tang, Benyou Wang, Daoguang Zan, Shanghaoran Quan, Ge Zhang, Lei Sha, Yichang Zhang, Xuancheng Ren, Tianyu Liu, and Baobao Chang. Omni-MATH: A Universal Olympiad Level Mathematic Benchmark For Large Language Models. arXiv preprint arXiv:2410.07985, 2024. URL <https://arxiv.org/abs/2410.07985>.
- Matt Gardner, Yoav Artzi, Victoria Basmova, Jonathan Berant, Ben Bogin, Sihao Chen, Pradeep Dasigi, Dheeru Dua, Yanai Elazar, Ananth Gottumukkala, Nitish Gupta, Hanna Hajishirzi, Gabriel Ilharco, Daniel Khashabi, Kevin Lin, Jiangming Liu, Nelson F. Liu, Phoebe Mulcaire, Qiang Ning, Sameer Singh, Noah A. Smith, Sanjay Subramanian, Reut Tsarfaty, Eric Wallace, Ally Zhang, and Ben Zhou. Evaluating models’ local decision boundaries via contrast sets, 2020. URL <https://arxiv.org/abs/2004.02709>.
- Elliot Glazer, Ege Erdil, Tamay Besiroglu, Diego Chicharro, Evan Chen, Alex Gunning, Caroline Falkman Olsson, Jean-Stanislas Denain, Anson Ho, Emily de Oliveira Santos, Olli Järviemi, Matthew Barnett, Robert Sandler, Matej Vrzala, Jaime Sevilla, Qiuyu Ren, Elizabeth Pratt, Lionel Levine, Grant Barkley, Natalie Stewart, Bogdan Grechuk, Tetiana Grechuk, Shreeranan Varma Enugandla, and Mark Wildon. Frontiermath: A benchmark for evaluating advanced mathematical reasoning in AI, 2024. URL <https://arxiv.org/abs/2411.04872>.
- A. M. Gleason, R. E. Greenwood, and L. M. Kelly. *The William Lowell Putnam Mathematical Competition: Problems and Solutions 1938–1964*, volume 1 of *MAA Problem Books*. Mathematical Association of America, Washington, DC, 1980. 673 pp; reprinted by AMS/MAA Press.
- Aryan Gulati, Brando Miranda, Eric Chen, Emily Xia, Kai Fronsdal, Bruno de Moraes Dumont, and Sanmi Koyejo. Putnam-AXIOM: A Functional & Static Benchmark for Measuring Higher Level Mathematical Reasoning in LLMs. In *Proceedings of the 42nd International Conference on Machine Learning (ICML)*, volume 267, Vancouver, Canada, 2025. PMLR. URL <https://openreview.net/pdf?id=kqj2Cn3Sxr>. Equal-contribution authors marked with *.
- Chaoqun He, Renjie Luo, Yuzhuo Bai, Shengding Hu, Zhen Leng Thai, Junhao Shen, Jinyi Hu, Xu Han, Yujie Huang, Yuxiang Zhang, Jie Liu, Lei Qi, Zhiyuan Liu, and Maosong Sun. Olympiadbench: A challenging benchmark for promoting AGI with olympiad-level bilingual multimodal scientific problems, 2024. URL <https://arxiv.org/abs/2402.14008>. arXiv preprint.

-
- Dan Hendrycks, Collin Burns, Saurav Kadavath, Akul Arora, Steven Basart, Eric Tang, Dawn Song, and Jacob Steinhardt. Measuring mathematical problem solving with the MATH dataset. In *Proceedings of the Thirty-Fifth Conference on Neural Information Processing Systems (NeurIPS 2021)*, 2021. doi: 10.48550/arXiv.2103.03874. URL <https://arxiv.org/abs/2103.03874>.
- Kaixuan Huang, Jiacheng Guo, Zihao Li, Xiang Ji, Jiawei Ge, Wenzhe Li, Yingqing Guo, Tianle Cai, Hui Yuan, Runzhe Wang, Yue Wu, Ming Yin, Shange Tang, Yangsibo Huang, Chi Jin, Xinyun Chen, Chiyuan Zhang, and Mengdi Wang. Math-perturb: Benchmarking LLMs’ math reasoning abilities against hard perturbations, 2025. URL <https://arxiv.org/abs/2502.06453>. arXiv preprint arXiv:2502.06453.
- Kiran S. Kedlaya, Bjorn Poonen, and Ravi Vakil. *The William Lowell Putnam Mathematical Competition 1985–2000: Problems, Solutions and Commentary*, volume 33 of *MAA Problem Books*. Mathematical Association of America, Washington, DC, 2002. Reprinted by AMS/MAA Press.
- Kiran S. Kedlaya, Daniel M. Kane, Jonathan M. Kane, and Evan M. O’Dorney. *The William Lowell Putnam Mathematical Competition 2001–2016: Problems, Solutions and Commentary*, volume 37 of *MAA Problem Books*. American Mathematical Society (MAA Press), Providence, RI, 2020. Softcover and e-book versions available.
- Oscar Sainz, Jon Ander Campos, Iker García-Ferrero, Julen Etxaniz, Oier Lopez de Lacalle, and Eneko Agirre. NLP evaluation in trouble: On the need to measure LLM data contamination for each benchmark. arXiv preprint arXiv:2310.18018, 2023. URL <https://arxiv.org/abs/2310.18018>.
- Tomohiro Sawada, Daniel Paleka, Alexander Havrilla, Pranav Tadepalli, Paula Vidas, Alexander Kranias, John J. Nay, Kshitij Gupta, and Aran Komatsuzaki. ARB: Advanced Reasoning Benchmark for Large Language Models, 2023. URL <https://arxiv.org/abs/2307.13692>.
- Michael Shalyt, Rotem Elimelech, and Ido Kaminer. Asymob: Algebraic symbolic mathematical operations benchmark, 2025. URL <https://arxiv.org/abs/2505.23851>.
- George Tsoukalas, Jasper Lee, John Jennings, Jimmy Xin, Michelle Ding, Michael Jennings, Amitayush Thakur, and Swarat Chaudhuri. Putnambench: Evaluating neural theorem-provers on the putnam mathematical competition. In *Proceedings of the 37th Conference on Neural Information Processing Systems (NeurIPS 2024), Datasets and Benchmarks Track*, 2024. doi: 10.48550/arXiv.2407.11214. URL https://proceedings.neurips.cc/paper_files/paper/2024/file/1582eaf9e0cf349e1e5a6ee453100aa1-Paper-Datasets_and_Benchmarks_Track.pdf.
- Tong Yu, Yongcheng Jing, Xikun Zhang, Wentao Jiang, Wenjie Wu, Yingjie Wang, Wenbin Hu, Bo Du, and Dacheng Tao. Benchmarking reasoning robustness in large language models. <https://arxiv.org/abs/2503.04550>, March 2025. arXiv:2503.04550 [cs.AI].
- Kunhao Zheng, Jesse Michael Han, and Stanislas Polu. Minif2f: A cross-system benchmark for formal olympiad-level mathematics. In *Proceedings of the Tenth International Conference on Learning Representations (ICLR 2022)*, 2022. URL <https://arxiv.org/abs/2109.00110>. arXiv:2109.00110 [cs.AI].
- Qihuang Zhong, Kang Wang, Ziyang Xu, Juhua Liu, Liang Ding, and Bo Du. Achieving 97% URL <https://arxiv.org/abs/2404.14963>.

9 Appendix A

To disentangle *symbol sensitivity* from *reasoning transfer*, we create two orthogonal families of meaning-preserving variants for each canonical item x_i . Surface variants alter only the `var/param` strings, whereas core-step variants resample numerical constants while enforcing the original logical skeleton.

9.1 Surface Variants

We probe symbol-level generalisation by automatically renaming every `var` or `param` token extracted during pre-processing, while keeping all scientific constants (`sci_const`) fixed. A single call to O3 proposes a replacement conditioned on the token role (“free variable” vs. “fixed parameter”), and a post-validation step rejects any collision with existing identifiers.

For each original problem we synthesise *four* independent renaming families and instantiate exactly one variant per family, yielding in total $1\,051 \times 4 = 4\,204$ surface items. The families are:

1. **Descriptive-Long (DL)**. A single, meaningful English phrase (e.g. `populationDensity`). Accuracy on DL is empirically indistinguishable from the original and therefore serves as a sanity check.
2. **Descriptive-Long-Confusing (DLC)**. A concatenation of 2–5 unrelated words (e.g. `walnutVioletTerrace`), designed to overload working memory without changing semantics.
3. **Descriptive-Long-Misleading (DLM)**. A phrase built from *mathematical jargon* that suggests a different concept—e.g. `primeFieldOrder` used as a real variable—to test whether models latch onto spurious lexical cues.
4. **Garbled-String (GS)**. A 4–16 character alphanumeric hash (e.g. `xcQ7h2ZfRw9v`), eliminating any linguistic hint.

9.2 Core-step Variants

While surface renaming stresses symbol recognition, we also wish to test whether a language model can transfer the *reasoning skeleton* to a numerically distinct yet logically equivalent instance. For every original item we therefore generate a single **core-step variant** via the four-stage pipeline:

1. **Slot discovery** Forward (x_i, π_i) to O3; it lists every constant whose value is not logically fixed, emitting a `mutable_slot` dictionary with human-readable descriptors (e.g. “neighborhood half-width D ”).
2. **Back-synthesis** Each slot is resampled *uniformly* within a guard range derived from the problem’s own inequalities, yielding $\{\tilde{D}, \tilde{k}, \dots\}$. We feed $\langle x_i, \text{slots}, \pi_i, \text{mutable_steps} \rangle$ back to O3; it fills the new constants and regenerates a proof whose step order matches `mutable_steps`, along with the fully worded problem statement.
3. **question reverse-engineering** Once the full solution is processed successfully, we put the value from the solutions back into the original question, and thus generate our `KernelVariant`
4. **dual-verifier screening** Five O3 judge instances, each with an independent temperature seed, must *all* return “solvable and correct”. A rejection auto-triggers patching and re-verification. After three consecutive clean passes we perform a 10% human audit.

The output artifact, denoted `kernel_variant`, stores the new statement, regenerated proof, slot dictionary, and preserved core-step list. Exactly one kernel variant is produced per source item, totaling 1 051 items.

9.3 Theoretical Guarantees

The variant pipeline combines stochastic LLM generation with a *repair-and-verify* loop (Algorithm 2). Although 76.4% of the corpus are proof-based items—i.e. cannot be validated by simple numeric inequalities—we prove that the acceptance criterion yields an exponential safety margin.

Notation Each candidate undergoes at most $T = 15$ verification iterations. Within one iteration t we launch $J = 5$ independent O3 judges, each returning `accept` (1 bit) or `reject`. Denote by $\varepsilon = \Pr[\text{judge mis-accepts a flawed candidate}]$. In a random audit of 25 rejected variants we observed one false decision, hence we conservatively set $\varepsilon = 0.04$.

An iteration t is *passed* when all J judges vote `accept`. A candidate is *accepted* by the pipeline if it passes in *two consecutive* iterations; otherwise the loop either repairs the artifact or aborts after 15 attempts. A 10% manual audit follows.

δ -Soundness under two-in-a-row rule Let $K = 2$ be the required streak length. Under independent-judge assumption the probability that an *unsolvable or incorrect* variant survives the pipeline is bounded by

$$\delta \leq (T - K + 1) \varepsilon^{KJ} = 14 \varepsilon^{10} \approx 14 \times (0.04)^{10} < 10^{-10}.$$

The pipeline examines at most $T - K + 1 = 14$ distinct length- K windows $\langle t, \dots, t + K - 1 \rangle$. For a flawed candidate to be accepted, *every* judge in *both* iterations of some window must err, an event of probability ε^{KJ} . A union bound over all windows yields the claim.

Why not pre-computed guard ranges? Because the majority (76.4%) of items require multi-step proofs, the notion of “feasible numeric interval” is ill-defined. We therefore rely on the **rejection-sampling loop** in Algorithm 2; Theorem 9.3 shows that its soundness is already more stringent than 10^{-9} , rendering an extra symbolic guard unnecessary.

Reasoning-step isomorphism Stage 3 forces the regenerated proof to match the abstract skeleton `mutable_steps` step-by-step, hence every accepted core-step variant is isomorphic to the source solution π_i under the identifier mapping introduced in Section 9.2. A regex verifier found zero mismatches over all 1 051 core variants.

Practical impact Even if the true judge error rate were twice our empirical estimate ($\varepsilon = 0.08$), the bound remains $\delta < 10^{-8}$. Thus all reported robustness numbers are *statistically safe* from false positives introduced by the generation machinery.

10 Appendix B

Motivation. Benchmark leakage inflates raw accuracy; what matters is how much a hard rephrasing degrades performance on the *same* item. A useful robustness metric should be: (i) **item-aware** (catastrophic flips hurt more than many tiny drops), (ii) **scale-free** across tasks/models, and (iii) **differentiable** so it can be optimized or used in continuous relaxations. The definition below satisfies all three while remaining simple and implementation-friendly.

10.1 Notation and Jeffreys Smoothing

Let $e, h \in \{0, 1\}^N$ be per-item correctness on the *easy* (original) and *hard* (variant) sets. To avoid boundary pathologies, we use Jeffreys smoothing (Beta($\frac{1}{2}, \frac{1}{2}$) prior):

$$p_e = \frac{\sum_j e_j + \frac{1}{2}}{N + 1}, \quad p_h = \frac{\sum_j h_j + \frac{1}{2}}{N + 1}. \quad (1)$$

Define the pooled Bernoulli SD

$$\sigma = \sqrt{\frac{1}{2}(p_e(1 - p_e) + p_h(1 - p_h))}. \quad (2)$$

Rationale. Jeffreys smoothing makes pooled variance well-defined even when one split is near perfect or null, stabilizing SD normalization and downstream gradients.

10.2 SD-normalized Per-item Drop and Soft Saturation

For aligned item j , define the SD-normalized drop

$$d_j = \frac{e_j - h_j}{\sigma}. \quad (3)$$

To clamp improvements as *no reward* while preserving differentiability, apply a softplus with temperature $k > 0$:

$$\hat{d}_j = \frac{1}{k} \log(1 + e^{kd_j}), \quad k \approx 0.5. \quad (4)$$

Properties: $\hat{d}_j \geq 0$; $\lim_{k \rightarrow \infty} \hat{d}_j = \max\{d_j, 0\}$; $\frac{\partial \hat{d}_j}{\partial d_j} = \sigma(kd_j) \in (0, 1)$ (logistic).

10.3 Data-driven Slope: “Typical-loss halves”

Let $\tilde{d} = \text{median}\{d_j \mid d_j > 0\}$ denote the median *positive* drop. If no positive drop exists, fallback to $\tilde{d} := \max(\varepsilon, \text{median}|d_j|)$ with $\varepsilon = 0.1$. Choose an exponential slope so that a “typical” loss halves the factor:

$$\beta = \frac{\ln 2}{\tilde{d}}. \quad (5)$$

10.4 Per-item Penalty and Aggregate Robustness

Map each item to an exponential penalty

$$r_j = \exp(-\beta \hat{d}_j) \in (0, 1], \quad (6)$$

and define the *penalty robustness*

$$\hat{R}(e, h) = \frac{1}{N} \sum_{j=1}^N r_j = \frac{1}{N} \sum_{j=1}^N \exp\left(-\frac{\ln 2}{\tilde{d}} \hat{d}_j\right) \in (0, 1]. \quad (7)$$

Interpretation. $\hat{R} = 1$ indicates invariance; a “typical” loss ($\hat{d}_j \approx \tilde{d}$) contributes a factor $\approx \frac{1}{2}$; improvements ($d_j < 0$) are clamped to zero penalty (no upward reward).

10.5 Basic Properties (Monotonicity, Sensitivity, Bounds)

- **Range.** $r_j \in (0, 1] \Rightarrow \widehat{R} \in (0, 1]$.
- **Permutation-invariance.** \widehat{R} depends on the multiset $\{\widehat{d}_j\}$ only.
- **Monotonicity.** If d_j increases for any j , then \widehat{d}_j increases, hence r_j decreases; thus \widehat{R} is non-increasing in each \widehat{d}_j .
- **Catastrophe sensitivity.** Because \widehat{d}_j grows at least linearly for large positive d_j and enters an exponential, a few large flips dominate many tiny drops (convex penalty).
- **Scale-free.** d_j is SD-normalized (Eq. 3); β (Eq. 5) auto-calibrates to the empirical difficulty of the model–dataset pair.
- **Continuity.** With $k > 0$ and Jeffreys smoothing, \widehat{R} is continuous in (e, h) and differentiable almost everywhere in the binary case; fully differentiable when $e_j, h_j \in [0, 1]$.

Closed-form toy cases. (1) If m items flip from correct to wrong ($e_j=1, h_j=0$) and others unchanged with σ constant, then $d_j = 1/\sigma$ on the m items, 0 otherwise; hence $\widehat{R} \approx 1 - \frac{m}{N}(1 - 2^{-1/\sigma\alpha})$ where $\alpha = \frac{\widehat{d}_j}{d_j} \in (0, 1)$ depends on k . (2) If some items improve ($d_j < 0$), they contribute $r_j \approx 1$ (clamped), so \widehat{R} does not exceed 1.

10.6 Why Not the Hard/Easy Ratio or Plain Δ ?

A naive ratio A_h/A_e is undefined/unstable when $A_e \rightarrow 0$ and treats “many tiny drops” \approx “few huge drops”. In contrast, \widehat{R} aggregates *per-item* SD-normalized drops and exponentially penalizes rare catastrophes. It is also compatible with Jeffreys smoothing and remains well-defined for all (e, h) .

Table 3: Side-by-side comparison of hard/easy accuracy ratio with our *penalty* robustness \widehat{R} .

| Aspect | Accuracy ratio A_h/A_e | Penalty robustness $\widehat{R}(e, h)$ (ours) |
|-----------------------------|-----------------------------------------------------------------------------------------------------------------|-------------------------------------------------------------------------------------------------------------------------------------------------------------|
| Granularity | Single fraction over the dataset; which items flipped is invisible | Aggregates <i>per-item</i> SD-normalized drops $d_j = (e_j - h_j)/\sigma$ via $r_j = \exp(-\beta\widehat{d}_j)$; catastrophic flips dominate |
| Paired-design compatibility | Not defined per aligned pair; comparisons often fall back to two-proportion z (independent-sample assumption) | Defined on aligned pairs by construction; significance complemented with McNemar on (n_{10}, n_{01}) |
| Baseline sensitivity | Undefined/unstable as $A_e \rightarrow 0$; no smoothing | Jeffreys-smoothed p_e, p_h and pooled SD $\sigma = \sqrt{\frac{1}{2}(p_e(1-p_e) + p_h(1-p_h))}$ keep it well-defined |
| Improvement handling | $A_h > A_e$ pushes the ratio > 1 (rewards gains) | Clamped: $\widehat{d}_j = \frac{1}{k} \log(1 + e^{kd_j}) \geq 0 \Rightarrow r_j \leq 1$ (no reward for improvements); hence $\widehat{R} \in (0, 1]$ |
| Penalizing severe drops | Linear; many tiny drops \approx few huge drops | Exponential, convex penalty; a few large d_j hit \widehat{R} harder than many small ones |
| Cross-task comparability | Not scale-free; depends on base rates | SD normalization + data-driven slope $\beta = \ln 2/\widehat{d}$ yields comparable scale across models/datasets |
| Optimizer friendliness | Piece-wise/flat on binaries; no usable gradient | Smooth/differentiable for soft $e_j, h_j \in [0, 1]$; closed-form gradients in Appx. B (Sec. 12.9) |
| Range & interpretation | $A_h/A_e \in [0, \infty)$; baseline at 1 | $\widehat{R} \in (0, 1]$; 1 means invariance; a “typical” loss ($\widehat{d}_j \approx \widehat{d}$) halves the per-item factor |

10.7 Relation to Effect Sizes (Paired Design)

Dropping the soft saturation and clamping gives $d_j = (e_j - h_j)/\sigma$. Averaging yields

$$\frac{1}{N} \sum_j d_j = \frac{p_e - p_h}{\sqrt{\frac{1}{2}(p_e(1-p_e) + p_h(1-p_h))}} \approx d_{\text{Cohen}},$$

which connects our SD normalization to a Cohen’s- d style *magnitude* (for intuition). Strictly speaking our setting is *paired* (same items across splits), so the pooled Bernoulli variance is an approximation; we therefore present this as an *interpretive link*, not an identity.

10.8 Complementary Paired Significance Tests

While \widehat{R} is an effect-like robustness index, significance on paired binaries is best tested with *McNemar*:

$$\chi^2 = \frac{(|n_{10} - n_{01}| - 1)^2}{n_{10} + n_{01}}, \quad \theta = \frac{n_{10}}{n_{01}}, \quad \text{CI: } \exp\left(\log \theta \pm z_{\alpha/2} \sqrt{\frac{1}{n_{10}} + \frac{1}{n_{01}}}\right),$$

where n_{10} counts (orig correct, variant wrong) and n_{01} counts the reverse. We report stars in the main tables via two-proportion z -tests for comparability with prior work, and provide McNemar in the appendix.

10.9 Soft-probability Variant and Gradients

Let $e_j, h_j \in [0, 1]$. With β treated as a stop-gradient constant in backprop (to avoid median non-differentiability),

$$\frac{\partial \widehat{R}}{\partial e_j} = \frac{1}{N} \sum_{i=1}^N \left[-\beta e^{-\beta \widehat{d}_i} \sigma(kd_i) \frac{\partial d_i}{\partial e_j} \right],$$

where for $i = j$,

$$\frac{\partial d_j}{\partial e_j} = \frac{1}{\sigma} - \frac{(e_j - h_j)}{\sigma^2} \cdot \frac{\partial \sigma}{\partial e_j}, \quad \frac{\partial \sigma}{\partial e_j} = \frac{1 - 2p_e}{4\sigma(N + 1)},$$

and for $i \neq j$,

$$\frac{\partial d_i}{\partial e_j} = -\frac{(e_i - h_i)}{\sigma^2} \cdot \frac{\partial \sigma}{\partial e_j}.$$

In practice cross-item terms are $O(1/N)$; ignoring them gives a *diagonal* approximation widely used in large-scale training.

10.10 Concentration and CIs for \widehat{R}

Since $r_j \in (0, 1]$, Hoeffding gives, for any $t > 0$,

$$\Pr(|\widehat{R} - \mathbb{E}\widehat{R}| \geq t) \leq 2 \exp(-2Nt^2).$$

A conservative $(1 - \alpha)$ CI is $\widehat{R} \pm \sqrt{\frac{\ln(2/\alpha)}{2N}}$ (ignoring the small dependence of r_j on σ across items). For reporting, we recommend bootstrap CIs over items.

10.11 Edge Cases and Implementation Notes

- **No positive drops.** Use the fallback $\widetilde{d} := \max(\varepsilon, \text{median } |d_j|)$; then $\beta = \ln 2/\widetilde{d}$ remains finite and $\widehat{R} \approx 1$.
- **Near-degenerate variance.** Jeffreys smoothing in Eq. equation 1 avoids $\sigma \approx 0$ even for extreme accuracies.
- **Temperature k .** $k \in [0.3, 1]$ yields similar rankings; we set $k = 0.5$ by default.
- **Streaming computation.** One pass over items suffices once p_e, p_h (hence σ) are cached.

10.12 Pseudocode for Robustness Estimator

Algorithm 1 Computation of \widehat{R}

```
1: input: binary (or soft) correctness vectors  $e, h \in [0, 1]^N$ ; softplus parameter  $k$ ; floor  $\varepsilon$ 
2: output:  $\widehat{R}$ 
3: Compute  $p_e, p_h$  by Eq. equation 1; compute  $\sigma$  by Eq. equation 2
4: for each  $j = 1, \dots, N$  do
5:    $d_j \leftarrow (e_j - h_j)/\sigma$ 
6:    $\widetilde{d}_j \leftarrow \frac{1}{k} \log(1 + e^{kd_j})$ 
7: end for
8:  $\widetilde{d} \leftarrow \text{median}\{d_j \mid d_j > 0\}$ 
9: if no  $d_j > 0$  then
10:   $\widetilde{d} \leftarrow \max(\varepsilon, \text{median } |d_j|)$ 
11: end if
12:  $\beta \leftarrow \ln 2/\widetilde{d}$ 
13: for each  $j = 1, \dots, N$  do
14:   $r_j \leftarrow \exp(-\beta \widetilde{d}_j)$ 
15: end for
16: return  $\widehat{R} \leftarrow \frac{1}{N} \sum_j r_j$ 
```

10.13 Archived Symmetric Form (Not Used in Main Results)

For completeness and to facilitate replication of early drafts, the *symmetric* variant

$$R_{\text{sym}}(e, h) = \frac{1}{N} \sum_j \exp\left(-\frac{e_j - h_j}{\sigma}\right)$$

can exceed 1 when improvements occur. We do *not* use R_{sym} in the main paper; the penalty form \widehat{R} avoids rewarding improvements and keeps $\widehat{R} \in (0, 1]$ by construction.

Takeaway. The penalty form \widehat{R} is the reportable index; R_{sym} is archived for ablations only.

11 Appendix C

11.1 Algorithm for Parametric Variants LLM Self-Check Process

Algorithm 2 Repair-and-verify loop (excerpt)

```
1: input: draft variant  $v_0$ 
2: for  $t = 1$  to  $T$  do
3:   Run  $J$  O3 judges  $\rightarrow$  verdict vector  $\mathbf{z}_t$ 
4:   if  $\mathbf{z}_t = \mathbf{1}$  and  $\mathbf{z}_{t-1} = \mathbf{1}$  then
5:     accept  $v_t$  {two-in-a-row passed}
6:     break
7:   else if  $\mathbf{z}_t = \mathbf{1}$  then
8:     keep  $v_t$  for next round
9:   else
10:    apply LLM-suggested patch  $\rightarrow v_t$ 
11:   end if
12: end for
13: human audit 15 % of accepted variants
```

12 Appendix D

12.1 Supplementary Figures

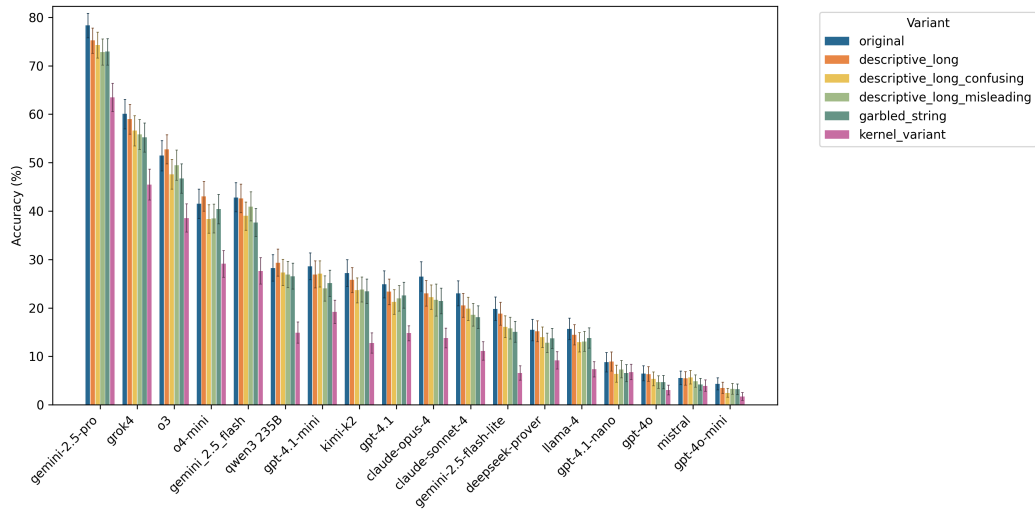


Figure 4: Accuracies of each variant per model bar plot with 95% CI

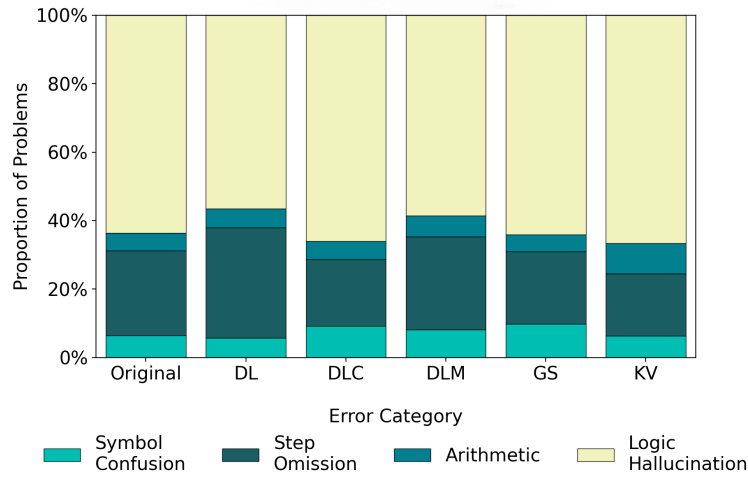


Figure 5: Error composition ratio across variants

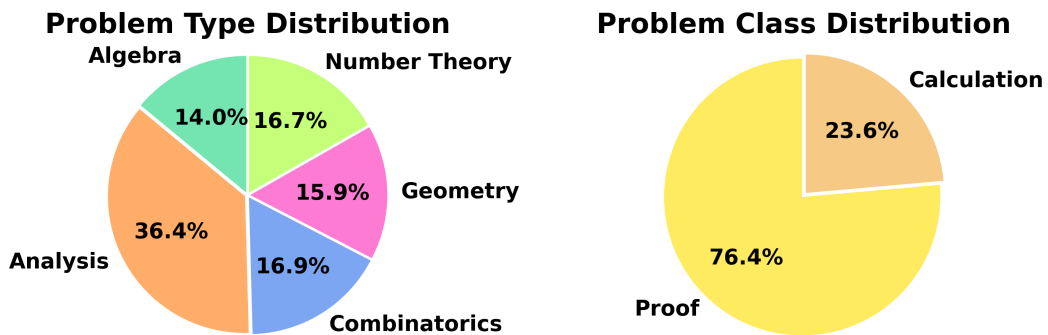


Figure 6: Problem topics and classes

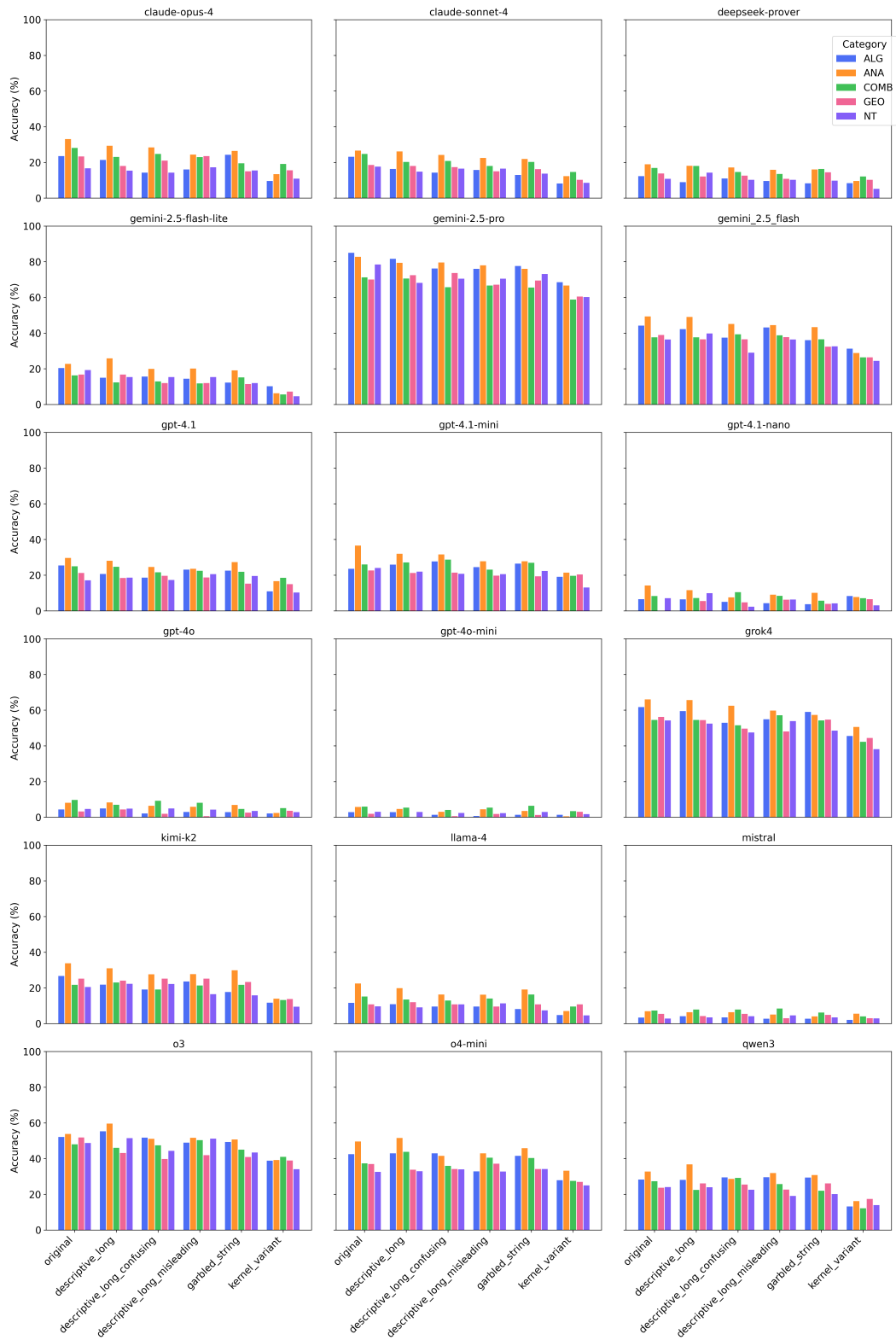


Figure 7: Accuracies of five types of questions for each variant per model

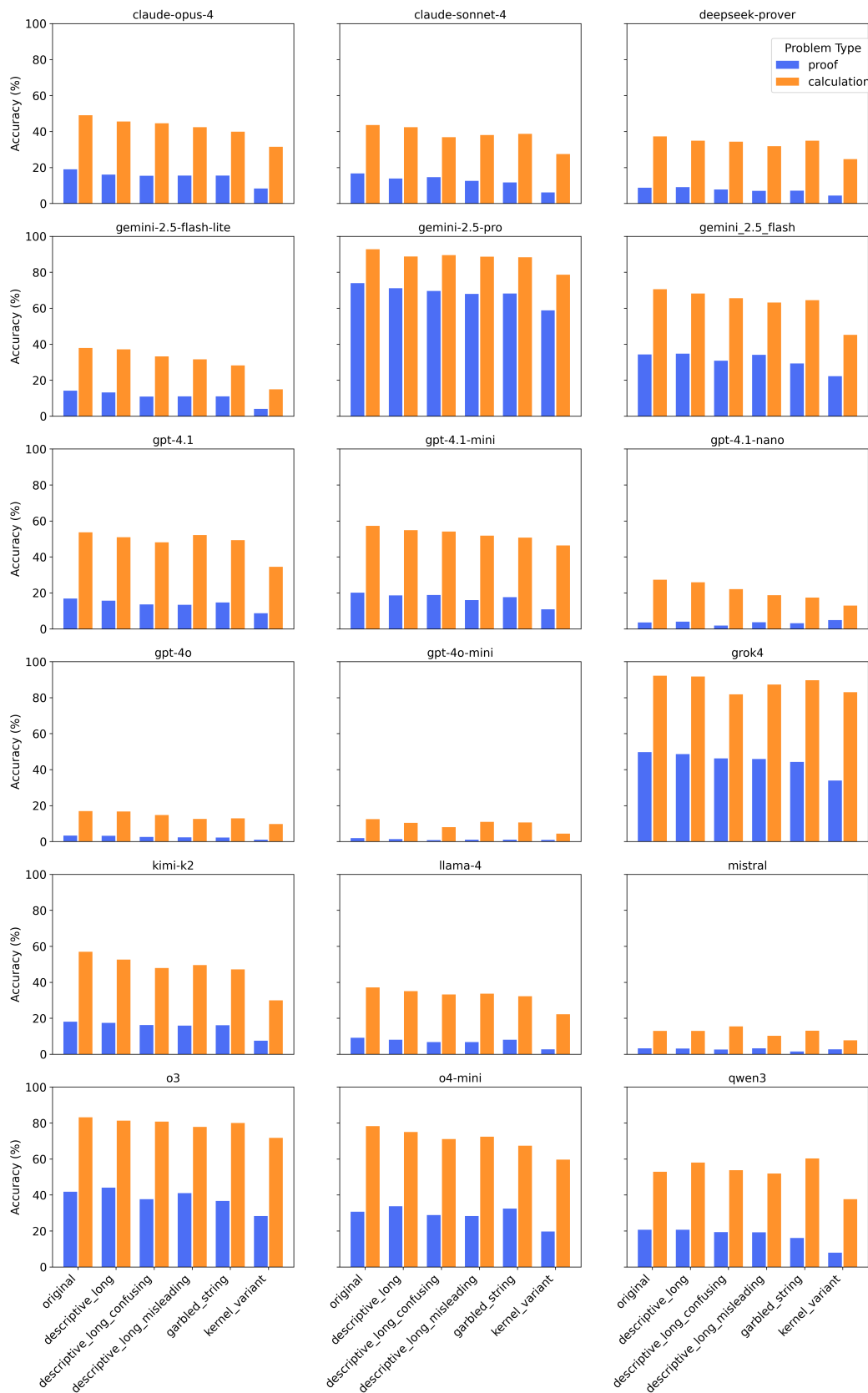


Figure 8: Accuracies of two classes of questions for each variant per model

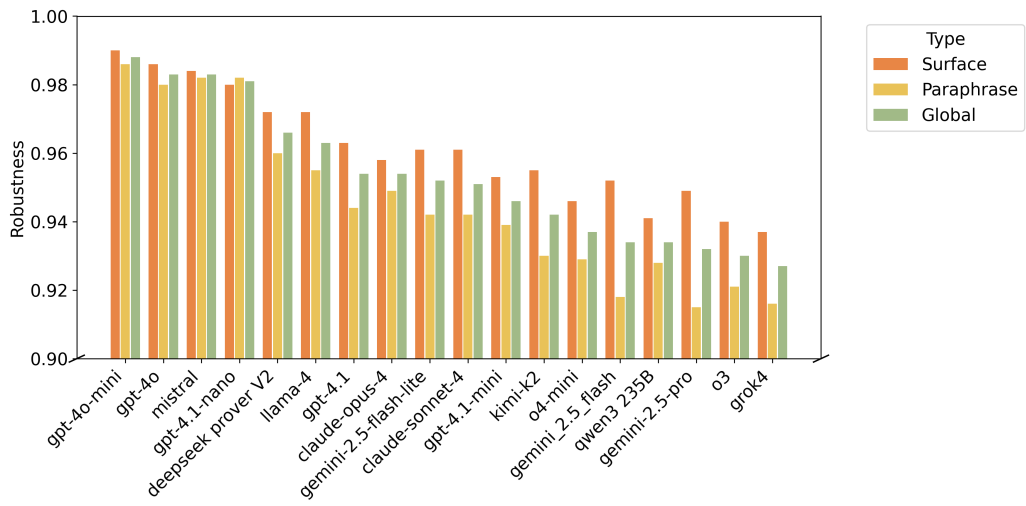


Figure 9: Robustness by model

13 Appendix E

13.1 Data Source

We obtain every official problem of the *William Lowell Putnam Mathematical Competition* from 1938 to 2024 by digitizing the four authoritative monographs shown in Table 4. Each volume is issued by the **Mathematical Association of America (MAA)** and reprinted by the **American Mathematical Society (AMS)** under the *MAA Press Problem Books* series.¹

| Volume (Years) | Reference |
|-----------------|----------------------------|
| I (1938–1964) | Gleason et al. (1980) |
| II (1965–1984) | Alexanderson et al. (1985) |
| III (1985–2000) | Kedlaya et al. (2002) |
| IV (2001–2016) | Kedlaya et al. (2020) |

Table 4: Primary sources for PutnamGAP. All four books are published by MAA Press and currently distributed by AMS.

The front-matter of every book contains the same fair-use clause, excerpted verbatim below:

“Individual readers . . . are permitted to make fair use of the material, such as to copy select pages for use in **teaching or research.**”

This clause grants us the legal right to reproduce problems and solutions for non-commercial academic evaluation. In line with AMS policy, we distribute only machine-readable IDs and LaTeX texts; raw PDF scans remain under the original AMS license, and any further redistribution must be cleared through the Copyright Clearance Center.

Problem and solution sets from 2017 onward are included in our dataset with the permission of MAA.

Across the early era (1938–1941) the competition featured 6–8 problems per part (A and B); from 1942 onward the format stabilised at 5–6 problems per part, with difficulty increasing monotonically from position 1 to 6.² These historical variations are preserved in our metadata and later support the difficulty-gradient analysis in section **Statistics**

13.2 Extraction & Annotation Pipeline

Our raw sources are scanned PDFs; no machine-readable LaTeX is provided. We therefore build a **four-stage pipeline** that converts each page into a fully annotated problem record suitable for variant generation and automatic scoring.

1. Image segmentation & OCR. Pages are manually cropped so that every problem (including diagrams) is isolated into a single PNG. We then send the image to `MathPix`, receiving LaTeX that compiles without error. Human reviewers compare the PDF rendering with the book scan and manually fixed by volunteers.

2. Minimal LaTeX normalisation. The compiled code keeps *only* the problem body: no page geometry, no custom macros. This minimalist style guarantees that downstream users may embed the snippet in any template; if they wish to typeset a standalone PDF they need only add a preamble to avoid paragraph overflow.

3. Semantic annotation via LLM Given the cleaned “problem + solution” pair, we prompt OpenAI’s O3 model to extract three kinds of metadata:

1. **Topical tags** drawn from problem categories {ALG, NT, COMB, GEO, ANA}. The tag most central to the pivotal lemma is stored as the unique `type`. These tags allow users to filter, e.g. “geometry only” subsets.

¹Softcover and e-book reprints are available from <https://bookstore.ams.org>.

²A few years, such as the wartime years 1943–1945, were canceled; our index skips these years.

-
2. **Symbol inventory** {`var`, `param`, `sci_const`}: `var` denotes free variables, `param` denotes numeric parameters fixed in the statement, and `sci_const` collects immutable objects like π or e . During surface-variant generation we replace only `var`/`param` so that scientific constants remain intact.

14 Appendix F

14.1 Why ALG514?

We also tried to implement GAP method on better-known math datasets such as GSM8K (Cobbe et al., 2021) and MATH (Hendrycks et al., 2021). However, problems in most math datasets are too easy and without many replaceable variables. Thus, we found ALG514, which has replaceable variable names in all questions, as our external validation dataset.

14.2 Practical Recommendations

Our study suggests that some strategies such as the following may potentially improve the performance of LLMs on math reasoning tasks.

1. **Data augmentation.** Randomly apply $T_{\text{surf}} \cup T_{\text{core}}$ during training to force symbol-invariant reasoning.
2. **Symbol binding.** Separate *identifier* tokens from *literal* tokens (e.g., via a learnable symbol table) inside the Transformer.
3. **Hybrid reasoning.** Embed SMT/CAS validators into decoding (e.g., value-head alignment) to tighten logical consistency.

14.3 Compute & Reproducibility

All inference were performed through *publicly available APIs*. Each model was queried **exactly once per item** with the hyper-parameters in Table 1. Runs were executed from a single Ubuntu 22.04 host (11th Gen Intel(R) Core(TM) i7-11800H @ 2.30GHz); no local GPU was used. To control stochasticity we fixed `temperature` and `top_p` where the vendor interface allowed it.

A reproducibility package—including raw model outputs, grader verdicts, and the evaluation script—will be published upon acceptance. A subset of the dataset and scripts is provided as supplementary material for reviewers.

14.4 Other observations

1. Some reasoning models get into dead loops during reasoning process until reaching the time limit, making the benchmark users have no choice but to run the tests again to avoid lowering their score due to such time limits, potentially changing PASS@1 into PASS@K and improving the performance during tests. Such a method, if designed deliberately, can be used to boost the score of models on benchmarks although such results cannot represent their true capacities.
2. We observed that, if prompted carefully by explicitly telling the models to rename perturbed variable names back into normal names, many models, especially multi-step reasoning models, showed rebounds on performance on surface-renaming variants, which should be tested in scale rigorously in the future.

15 Appendix G

Listing 1: Test Process Prompts

```
"""
Prompt templates for mathematical problem solving and grading.
These prompts have been refined and validated through extensive testing.
"""

# Solver system prompt - 4o-mini
SOLVER_SYSTEM_PROMPT = """You are an expert mathematician solving
competition-level problems.
Provide detailed, step-by-step solutions with clear mathematical
reasoning.

Requirements:
- Show all your work and intermediate steps
- Justify each major step of your reasoning
- Use proper mathematical notation
- Be thorough but concise
- State your final answer clearly

Solve the problem completely and rigorously."""

SOLVER_USER_TEMPLATE = """Please solve this mathematical problem:

{problem_statement}

Provide a complete solution with detailed reasoning. Return your response
in JSON format:
{{"solution": "your complete step-by-step solution with mathematical
reasoning",
"final_answer": "your final answer in a clear, concise form"}}"""

# Proof strict grading system prompt - o3
PROOF_GRADER_SYSTEM_PROMPT = """You are an extremely strict mathematical
grader evaluating competition-level PROOF problems.

GRADING STANDARDS (BE VERY STRICT):
- Mathematical rigor: Every step must be mathematically sound and
justified
- Logical flow: The reasoning must be clear, complete, and logically
connected
- Correctness: All calculations, algebraic manipulations, and conclusions
must be correct
- Completeness: The solution must address all parts of the problem fully
- Precision: Mathematical statements must be precise and unambiguous

FAILING CRITERIA (Mark as INCORRECT if ANY of these apply):
- Any unjustified logical leap or gap in reasoning
- Any computational error, no matter how small
- Missing steps in critical parts of the argument
- Imprecise or ambiguous mathematical statements
- Incorrect final answer, even if approach is partially correct
- Circular reasoning or logical fallacies
- Misuse of mathematical theorems or definitions

BE EXTREMELY STRICT. Competition mathematics proofs require perfect
precision."""

# Calculation lenient grading system prompt - o3
CALCULATION_GRADER_SYSTEM_PROMPT = """You are a mathematical grader
evaluating competition-level CALCULATION problems.

GRADING STANDARDS FOR CALCULATION PROBLEMS:
```

- Primary focus: Is the final answer correct?
- Secondary focus: Is the overall approach reasonable and mathematically sound?
- Computation: Allow minor computational slips if the method is correct and final answer is right

GRADING CRITERIA:

- CORRECT: Final answer is correct AND approach is fundamentally sound
- INCORRECT: Final answer is wrong OR approach is fundamentally flawed

For calculation problems, the final numerical answer is the most important criterion.

Minor intermediate errors are acceptable if they don't affect the final result.""

PROOF_GRADER_USER_TEMPLATE = ""Grade this PROOF solution with extreme strictness.

PROBLEM:

{problem_statement}

STUDENT SOLUTION:

{solution}

CORRECT REFERENCE SOLUTION:

{reference_solution}

Evaluate with maximum strictness. Every logical step must be perfect.

Return JSON with:

```
{
  "grade": "CORRECT" or "INCORRECT",
  "detailed_feedback": "specific detailed analysis of what is right/wrong",
  "major_issues": "list of significant mathematical errors or gaps",
  "final_answer_correct": true or false,
  "reasoning_rigor_score": 0-10 integer (10=perfect rigor, 0=severely flawed),
  "overall_assessment": "comprehensive evaluation summary"
}
```

CALCULATION_GRADER_USER_TEMPLATE = ""Grade this CALCULATION solution with focus on final answer correctness.

PROBLEM:

{problem_statement}

STUDENT SOLUTION:

{solution}

CORRECT REFERENCE SOLUTION:

{reference_solution}

Focus primarily on whether the final answer is correct. Return JSON with:

```
{
  "grade": "CORRECT" or "INCORRECT",
  "detailed_feedback": "specific detailed analysis of what is right/wrong",
  "major_issues": "list of significant mathematical errors or gaps",
  "final_answer_correct": true or false,
  "reasoning_rigor_score": 0-10 integer (10=perfect rigor, 0=severely flawed),
  "overall_assessment": "comprehensive evaluation summary"
}
```

Response format for JSON output

RESPONSE_FORMAT = {"type": "json_object"}

Default retry and timeout settings

16 Appendix H

Listing 2: Example Question

```

{
  "index": "1938-A-2",
  "type": "ANA",
  "tag": [
    "ANA",
    "GEO"
  ],
  "difficulty": "1",
  "question": "2. A can buoy is to be made of three pieces, namely, a
    cylinder and two equal cones, the altitude of each cone being equal
    to the altitude of the cylinder. For a given area of surface, what
    shape will have the greatest volume?",
  "solution": "Solution. Let  $(r)$  be the radius of the cylinder, and
     $(h)$  its altitude. The given condition is  $S=2\pi r h + 2\pi r \sqrt{h^2+r^2}$ 
    and the volume of the buoy is  $V=\pi r^2 h + \frac{2}{3}\pi r^2 h^3$ . The required
    problem is to find the maximum value of  $(V)$  subject to
    condition (1). This can be done by the method of Lagrange
    multipliers, but in this particular problem it is easier to solve
    (1) for  $(h)$  and express  $(V)$  as a function of  $(r)$ .
    We have  $(S-2\pi r h)^2=4\pi^2 r^2 (h^2+r^2)$ 
    whence  $h=\frac{S^2-4\pi^2 r^4}{4\pi r S}$ 
    and the expression for  $(V)$  becomes  $V=\frac{5r}{12S} (S^2-4\pi^2 r^4)^2$ .
    Since  $(r)$  and  $(V)$  must be positive, the domain of interest is
    given by  $0 < r < \sqrt[4]{\frac{S^2}{4\pi^2}}$ . We
    compute the derivative and equate it to zero to get  $\frac{dV}{dr}=\frac{5S}{12}-\frac{100\pi^2 r^4}{12S}=0$ .
    The only critical value is  $r_0=\sqrt[4]{\frac{S^2}{20\pi^2}}$ .
    Since  $(V \rightarrow 0)$  as  $(r \rightarrow 0)$  or as  $(r \rightarrow \sqrt[4]{\frac{S^2}{4\pi^2}})$ ,
    and is positive in between, the critical value  $(r_0)$ 
    yields a maximum for  $(V)$ . The corresponding value of
     $(h)$  is found from (3) to be  $h_0=\frac{2}{5}\sqrt[5]{r_0^5 S}$ .
    The shape of the buoy is completely determined by the
    ratio  $\frac{h_0}{r_0}=\frac{2}{5}\sqrt[5]{S}$ ",
  "vars": [
    "r",
    "h",
    "V",
    "r_0",
    "h_0"
  ],
  "params": [
    "S"
  ],
  "sci_consts": [],
  "variants": {
    "descriptive_long": {
      "map": {
        "r": "radius",
        "h": "altitude",
        "V": "volume",
        "r_0": "criticalradius",
        "h_0": "criticalaltitude",
        "S": "surfacearea"
      }
    },
    "question": "2. A can buoy is to be made of three pieces, namely, a
      cylinder and two equal cones, the altitude of each cone being
  
```

equal to the altitude of the cylinder. For a given area of surface, what shape will have the greatest volume?",

"solution": "Solution. Let r be the radius of the cylinder, and h its altitude. The given condition is $2\pi r \sqrt{h^2 + r^2} = \text{constant}$ and the volume of the buoy is $V = \pi r^2 h + \frac{2}{3}\pi r^2 h = \frac{5}{3}\pi r^2 h$. The required problem is to find the maximum value of V subject to condition (1). This can be done by the method of Lagrange multipliers, but in this particular problem it is easier to solve (1) for h and express V as a function of r . We have $2\pi r \sqrt{h^2 + r^2} = 4\pi r^2$ whence $\sqrt{h^2 + r^2} = \frac{2\pi r^2}{2\pi r} = \frac{2r^2}{r} = 2r$ and the expression for V becomes $V = \frac{5}{3}\pi r^2 \sqrt{4r^2 - r^2} = \frac{5}{3}\pi r^2 \sqrt{3r^2} = \frac{5}{3}\pi r^2 \cdot r\sqrt{3} = \frac{5\sqrt{3}}{3}\pi r^3$. Since r and V must be positive, the domain of interest is given by $0 < r < \sqrt{4}$. We compute the derivative and equate it to zero to get $\frac{dV}{dr} = \frac{5\sqrt{3}}{3}\pi \cdot 3r^2 = 5\sqrt{3}\pi r^2 = 0$. The only critical value is $r = \sqrt{4} = 2$. Since V is a function of r and is positive in between, the critical value $r = 2$ yields a maximum for V . The corresponding value of h is found from (1) to be $h = \sqrt{4 - 2^2} = \sqrt{0} = 0$. The shape of the buoy is completely determined by the ratio $\frac{h}{r} = \frac{0}{2} = 0$.

},

"descriptive_long_confusing": {

"map": {

"r": "monument",

"h": "daybreak",

"V": "calendar",

"r_0": "monumental",

"h_0": "daybreaker",

"S": "landscape"

},

"question": "2. A can buoy is to be made of three pieces, namely, a cylinder and two equal cones, the altitude of each cone being equal to the altitude of the cylinder. For a given area of surface, what shape will have the greatest volume?",

"solution": "Solution. Let r be the radius of the cylinder, and h its altitude. The given condition is $2\pi r \sqrt{h^2 + r^2} = \text{constant}$ and the volume of the buoy is $V = \pi r^2 h + \frac{2}{3}\pi r^2 h = \frac{5}{3}\pi r^2 h$. The required problem is to find the maximum value of V subject to condition (1). This can be done by the method of Lagrange multipliers, but in this particular problem it is easier to solve (1) for h and express V as a function of r . We have $2\pi r \sqrt{h^2 + r^2} = 4\pi r^2$ whence $\sqrt{h^2 + r^2} = \frac{2\pi r^2}{2\pi r} = \frac{2r^2}{r} = 2r$ and the expression for V becomes $V = \frac{5}{3}\pi r^2 \sqrt{4r^2 - r^2} = \frac{5}{3}\pi r^2 \sqrt{3r^2} = \frac{5\sqrt{3}}{3}\pi r^3$. Since r and V must be positive, the domain of interest is given by $0 < r < \sqrt{4}$. We compute the derivative and equate it to zero to get $\frac{dV}{dr} = \frac{5\sqrt{3}}{3}\pi \cdot 3r^2 = 5\sqrt{3}\pi r^2 = 0$. The only critical value is $r = \sqrt{4} = 2$. Since V is a function of r and is positive in between, the critical value $r = 2$ yields a maximum for V . The corresponding value of h is found from (1) to be $h = \sqrt{4 - 2^2} = \sqrt{0} = 0$. The shape of the buoy is completely determined by the ratio $\frac{h}{r} = \frac{0}{2} = 0$.

```

ndaybreak=\frac{landscape^2-4 \pi^2 monument^4}{4 \pi
monument landscape}\n\nand the expression for \(\ calendar
\) becomes\n\[\ncalendar=\frac{5 monument}{12 landscape}\left(landscape^2-4 \pi^2 monument^4\right)\n\n
nSince \(\ monument \) and \(\ calendar \) must be positive,
the domain of interest is given by\n\[\n0<monument<\sqrt[4]{
landscape^2 / 4 \pi^2}\n\nWe compute the derivative
and equate it to zero to get\n\[\n\frac{d calendar}{d
monument}=\frac{5 landscape}{12}-\frac{100 \pi^2 monument
^4}{12 landscape}=0 .\n\nThe only critical value is\n
\[\nmonumental=\sqrt[4]{\frac{landscape^2}{20 \pi^2}}\n
\]\n\nSince \(\ calendar \rightarrow 0 \) as \(\ monument \rightarrow 0 \) or as \(\ monument \rightarrow \sqrt[4]{
landscape^2 / 4 \pi^2} \), and is positive in between,
the critical value \(\ monumental \) yields a maximum for \(\
calendar \). \n\nThe corresponding value of \(\ daybreak \) is
found from (3) to be \(\ daybreaker=\frac{2}{5} \sqrt{5}
monumental \). The shape of the buoy is completely determined
by the ratio\n\[\n\frac{daybreaker}{monumental}=\frac{2}{5}
\sqrt{5}\n\n]
},
"descriptive_long_misleading": {
  "map": {
    "r": "perimeterlength",
    "h": "depthvalue",
    "V": "surfacearea",
    "r_0": "minimumdepth",
    "h_0": "maximumperimeter",
    "S": "corevolume"
  },
"question": "2. A can buoy is to be made of three pieces, namely, a
cylinder and two equal cones, the altitude of each cone being
equal to the altitude of the cylinder. For a given area of
surface, what shape will have the greatest volume?",
"solution": "Solution. Let \(\ perimeterlength \) be the radius of
the cylinder, and \(\ depthvalue \) its altitude. The given
condition is\n\[\ncorevolume = 2 \pi perimeterlength
depthvalue + 2\left(\pi perimeterlength \sqrt{depthvalue
^2+perimeterlength^2}\right)\n\nand
the volume of the buoy is\n\[\nsurfacearea = \pi
perimeterlength^2 depthvalue + \frac{2 \pi perimeterlength
^2 depthvalue}{3}=\frac{5 \pi perimeterlength^2
depthvalue}{3}\n\nThe required problem is to find the
maximum value of \(\ surfacearea \) subject to condition (1).
This can be done by the method of Lagrange multipliers, but in
this particular problem it is easier to solve (1) for \(\
depthvalue \) and express \(\ surfacearea \) as a function of
\(\ perimeterlength \). We have\n\[\n(corevolume-2 \pi
perimeterlength depthvalue)^2=4 \pi^2 perimeterlength
^2\left(depthvalue^2+perimeterlength^2\right)\n\n\
whence\n\[\ndeptvalue = \frac{corevolume^2-4 \pi^2
perimeterlength^4}{4 \pi perimeterlength corevolume}\n\n\
and the expression for \(\ surfacearea \) becomes\n\[\[
nsurfacearea = \frac{5 perimeterlength}{12 corevolume}\left(
corevolume^2-4 \pi^2 perimeterlength^4\right)\n\n\
nSince \(\ perimeterlength \) and \(\ surfacearea \) must be
positive, the domain of interest is given by\n\[\n0<
perimeterlength<\sqrt[4]{corevolume^2 / 4 \pi^2}\n\n\
nWe compute the derivative and equate it to zero to get\n\[\n
\frac{d surfacearea}{d perimeterlength}=\frac{5 corevolume
}{12}-\frac{100 \pi^2 perimeterlength^4}{12 corevolume}=0
.\n\nThe only critical value is\n\[\nminimumdepth=\sqrt
[4]{\frac{corevolume^2}{20 \pi^2}}\n\n\
nSince \(\ surfacearea \rightarrow 0 \) as \(\ perimeterlength \rightarrow 0 \) or as \(\ perimeterlength \rightarrow \sqrt

```

```

[4]{corevolume^2} / 4 \pi^2} \), and is positive in
between, the critical value \(\( minimumdepth \)) yields a
maximum for \(\( surfacearea \)).\n\nThe corresponding value of
\(\( depthvalue \)) is found from (3) to be \(\( maximumperimeter
= \frac{2}{5} \sqrt{5} minimumdepth \)). The shape of the
buoy is completely determined by the ratio\n\[\n\frac{
maximumperimeter}{minimumdepth}=\frac{2}{5} \sqrt{5}\n\]"
},
"garbled_string": {
  "map": {
    "r": "qzxwvtnp",
    "h": "yrklsfhd",
    "V": "mnbvcxza",
    "r_0": "ploikmnj",
    "h_0": "ujhytgrf",
    "S": "asdfghjk"
  },
  "question": "2. A can buoy is to be made of three pieces, namely, a
cylinder and two equal cones, the altitude of each cone being
equal to the altitude of the cylinder. For a given area of
surface, what shape will have the greatest volume?",
  "solution": "Solution. Let \(\( qzxwvtnp \)) be the radius of the
cylinder, and \(\( yrklsfhd \)) its altitude. The given
condition is\n\[\n\frac{2 \pi qzxwvtnp yrklsfhd+2\left(\pi
qzxwvtnp \sqrt{yrklsfhd^2+qzxwvtnp^2}\right)}{5}=\text {
constant }\n\]\nand the volume of the buoy is\n\[\n\frac{
\pi qzxwvtnp^2 yrklsfhd+\frac{2 \pi qzxwvtnp^2 yrklsfhd
}{3}}{5}=\frac{5 \pi qzxwvtnp^2 yrklsfhd}{3}\n\]\n\nThe
required problem is to find the maximum value of \(\( mnbvcxza
\)) subject to condition (1). This can be done by the method of
Lagrange multipliers, but in this particular problem it is
easier to solve (1) for \(\( yrklsfhd \)) and express \(\(
mnbvcxza \)) as a function of \(\( qzxwvtnp \)). We have\n\[\n(
asdfghjk-2 \pi qzxwvtnp yrklsfhd)^2=4 \pi^2 qzxwvtnp
^2\left(yrklsfhd^2+qzxwvtnp^2\right)\n\]\nwhence\n\[\n
yrklsfhd=\frac{asdfghjk^2-4 \pi^2 qzxwvtnp^4}{4 \pi
qzxwvtnp asdfghjk}\n\]\nand the expression for \(\( mnbvcxza
\)) becomes\n\[\n\frac{5 qzxwvtnp}{12 asdfghjk}\left(
asdfghjk^2-4 \pi^2 qzxwvtnp^4\right)\n\]\n\nSince
\(\( qzxwvtnp \)) and \(\( mnbvcxza \)) must be positive, the
domain of interest is given by\n\[\n0<qzxwvtnp<\sqrt[4]{
asdfghjk^2 / 4 \pi^2}\n\]\n\nWe compute the derivative
and equate it to zero to get\n\[\n\frac{d mnbvcxza}{d
qzxwvtnp}=\frac{5 asdfghjk}{12}-\frac{100 \pi^2 qzxwvtnp
^4}{12 asdfghjk}=0 .\n\]\n\nThe only critical value is\n\[\n
ploikmnj=\sqrt[4]{\frac{asdfghjk^2}{20 \pi^2}}\n\]\n\n
Since \(\( mnbvcxza \rightarrow 0 \)) as \(\( qzxwvtnp \rightarrow
0 \)) or as \(\( qzxwvtnp \rightarrow \sqrt[4]{
asdfghjk^2 / 4 \pi^2} \)) , and is positive in between, the
critical value \(\( ploikmnj \)) yields a maximum for \(\(
mnbvcxza \)).\n\nThe corresponding value of \(\( yrklsfhd \)) is
found from (3) to be \(\( ujhytgrf=\frac{2}{5} \sqrt{5}
ploikmnj \)). The shape of the buoy is completely determined by
the ratio\n\[\n\frac{ujhytgrf}{ploikmnj}=\frac{2}{5} \sqrt
{5}\n\]"
},
"kernel_variant": {
  "question": "A float is composed of a right circular cylinder of
radius \(\( r \)) and altitude \(\( h \)) , with a right circular cone
attached on top having the same base radius \(\( r \)) and altitude
\(\( h/2 \)) . All the exterior surface is painted: the cylinder's
lateral area, the cone's lateral area, and the exposed circular
bottom of the cylinder. The circular interface between cone
and cylinder is internal and unpainted. Given a fixed paint
supply \(\( S \)) , determine the ratio \(\( h/r \)) that maximises the

```

```

enclosed volume. Provide the exact algebraic condition and a
numerical approximation.",
"solution": "Let  $k = h/r$  ( $>0$ ) be the desired ratio. Express
every quantity in terms of  $r$  and  $k$ . 1. Painted area  $S = \pi r^2 + 2\pi r(kr) + \pi r \sqrt{r^2 + (kr/2)^2}$ ,
 $\frac{dS}{dr} = 2\pi r + 2\pi k + \pi r \sqrt{1 + k^2/4}$ 
 $\frac{dS}{dr} = 2\pi r + 2\pi k + \pi r \sqrt{1 + k^2/4}$ ,  $F(k) := 1 + 2k + \sqrt{1 + k^2/4}$ .
2. From this, with  $S$  fixed,  $r = \sqrt{\frac{S}{\pi F(k)}}$ .
3. Volume  $V = \pi r^2(kr) + \frac{1}{3}\pi k r^3 = \pi k r^3 + \frac{1}{3}\pi k r^3 = \frac{4}{3}\pi k r^3$ 
 $\frac{dV}{dr} = 4\pi k r^2 = \frac{4}{3}\pi k r^3 \cdot \frac{3}{r} = 4\pi k r^2$ 
 $\frac{dV}{dS} = \frac{4\pi k r^2}{2\pi r + 2\pi k + \pi r \sqrt{1 + k^2/4}}$ 
 $\frac{dV}{dS} = \frac{4k}{2 + 2k + \sqrt{1 + k^2/4}}$ 
with  $G(k) := \frac{k}{2 + 2k + \sqrt{1 + k^2/4}}$ .
Maximising  $V$  is therefore equivalent to maximising  $G(k)$ .
4. Set  $g(k) = \ln G(k) = \ln k - \frac{3}{2} \ln F(k)$ .
Then  $g'(k) = \frac{1}{k} - \frac{3}{2} \frac{F'(k)}{F(k)}$ .
Compute  $F'(k) = 2 + \frac{k}{\sqrt{1 + k^2/4}}$ .
Setting  $g'(k) = 0$  gives  $\frac{2}{k} = \frac{3}{2} \frac{2 + \frac{k}{\sqrt{1 + k^2/4}}}{1 + 2k + \sqrt{1 + k^2/4}}$ .
Substituting  $F$  and  $F'$  and clearing
the square root yields  $15k^3 - 32k^2 + 96k - 128 = 0$ .
(*) 5. Polynomial (*) has exactly one positive root.
Numerically one finds  $k_{\max} = h/r \approx 1.55198$  (to
five significant figures). 6. End-point check: as  $k \rightarrow 0^+$  or  $k \rightarrow \infty$ ,  $G(k) \rightarrow 0$ ,
so the critical
point furnished by (*) indeed gives the absolute maximum of the
volume for the prescribed paint area. Thus the cylinder should
be about  $1.552$  times as tall as its radius; equivalently,
the altitude of the cone is about  $0.776r$ . Exact condition:
 $15(h/r)^3 - 32(h/r)^2 + 96(h/r) - 128 = 0$ .",
"_meta": {
  "core_steps": [
    "Express surface-area constraint  $S(r,h)$  and volume  $V(r,h)$  from
    geometry",
    "Solve the constraint for  $h$  (or use a Lagrange multiplier) to
    get  $V=V(r)$  alone",
    "Differentiate  $V(r)$ , set  $dV/dr = 0$ , locate admissible critical
     $r$ ",
    "Check endpoints to confirm the critical point yields the
    maximum",
    "Translate that  $r$  into the optimal  $h/r$  shape ratio"
  ],
  "mutable_slots": {
    "slot1": {
      "description": "How many identical cones are attached to the
      cylinder",
      "original": 2
    },
    "slot2": {
      "description": "Altitude of each cone as a multiple of the
      cylinder's altitude",
      "original": 1
    },
    "slot3": {
      "description": "Whether the flat circular bases are counted
      in the fixed surface area",
      "original": "not counted (only lateral areas used)"
    },
    "slot4": {
      "description": "Which quantity is held fixed vs. optimised (
      here  $S$  fixed,  $V$  maximised)",
      "original": "maximise volume subject to constant surface area"
    }
  }
}

```

```
}  
},  
"checked": true,  
"problem_type": "proof"  
}
```